
Chapter 5 Induced Radioactivity at Accelerators

In this chapter the production of induced radioactivity at accelerators is described. This discussion begins with a review of the basic principles of the production of radioactivity. It proceeds with a discussion of the activation of accelerator components including some generalizations that may be used for practical health physics applications. The chapter also considers the production of airborne radioactivity from both the standpoints of occupational and environmental radiological protection. Finally, the chapter concludes with a discussion of soil and groundwater activation pertinent to the protection of the environment.

I. Fundamental Principles of Induced Radioactivity at Accelerators

In principle, induced radioactivity can be produced at all accelerators capable of liberating neutrons and other hadrons. When the accelerated beam strikes a nucleus, it converts it into a different nuclide which may be radioactive. In these discussions, the **activity** of a given radionuclide refers to the number of atoms that decay per unit time. The customary unit of activity is the **Curie** (and its submultiples) which was originally defined to be the activity of 1 gram of natural radium but now is precisely 3.7×10^{10} decays per second. The SI unit of activity is the **Becquerel**, and its multiples, which is defined to be 1 decay per second. A related quantity of considerable importance is the **specific activity** that is defined to be the activity per unit volume or, alternatively, the activity per unit mass.

Radioactive decay is a random process characterized by a **mean-life** (time) denoted by τ , and its reciprocal, the decay constant λ [$\lambda = 1/\tau$]¹. If a total of $N_{tot}(t)$ atoms of a radionuclide are present at time t , the total activity $A_{tot}(t)$ is determined by the random nature of radioactive decay to be

$$A_{tot}(t) = -\frac{dN_{tot}(t)}{dt} = -\frac{1}{\tau}N_{tot}(t) = -\lambda N_{tot}(t). \quad (5.1)$$

If, at time $t = 0$, $N_{tot}(0)$ atoms are present, then this simple differential equation has the solution at some time $t > 0$;

$$A_{tot}(t) = \lambda N_{tot}(0) \exp(-\lambda t) = A_{tot}(0) \exp(-\lambda t). \quad (5.2)$$

Often, the time required to decay to half of the original activity is tabulated. This **half-life**, denoted as $t_{1/2}$, is related to the mean-life by the following:

$$\tau = \frac{1}{\ln 2} t_{1/2} = \frac{1}{0.693} t_{1/2} = 1.442 t_{1/2}. \quad (5.3)$$

The most simple activation situation at accelerators is illustrated by the steady irradiation of some material by a spatially uniform flux density of particles that begins at some time $t = 0$, continues at a constant rate for an **irradiation period** that ends at $t = t_i$. This is followed by a decay period called the **cooling time** and denoted t_c . t_c is a period

¹ Care needs to be taken with respect to the usage of the symbol λ . In the literature and here it is used for both attenuation length and for the decay constant. The reader needs to take note of the context to apply the correct meaning.

Chapter 5 Induced Radioactivity at Accelerators

which begins at $t = t_i$ and ends at $t = t_i + t_c$. For this simple situation, self-absorption of the hadrons by the target is ignored. Ignored is the fact that a whole spectrum of neutrons might be present. Thus the process of producing the radioactivity is characterized by a single average cross section, σ , which, in the more complicated generalized situations must be obtained from averaging over a spectrum.

The number of atoms of the radionuclide of interest per unit volume will thus be governed by the following differential equation during the period of the irradiation:

$$\frac{dn(t)}{dt} = -\lambda n(t) + N\sigma\phi, \quad (5.4)$$

where $n(t)$ is the atoms of the radionuclide per cm^3 at time t . N is the number of "target" atoms per cm^3 , σ is in units of cm^2 , and ϕ is the flux density ($\text{cm}^{-2} \text{sec}^{-1}$) of incident particles. On the right hand side of the above equation, the first term represents the loss of radionuclides through decay during the irradiation while the second term represents the gain of radionuclides through the production reaction under consideration. The equation has the following solution for $0 < t < t_i$;

$$n(t) = \frac{N\sigma\phi}{\lambda} (1 - e^{-\lambda t}). \quad (5.5)$$

Thus the specific activity (Bq/cm^3) induced in the material as a function of time during the irradiation is given by $a(t) = \lambda n(t)$, hence

$$a(t) = N\sigma\phi (1 - e^{-\lambda t}) \quad \text{for } 0 < t < t_i. \quad (5.6)$$

To obtain specific activity in units of Curies/ cm^3 , one must simply divide by the conversion factor $3.7 \times 10^{10} \text{ Bq/Curie}$. At the instant of completion of the irradiation ($t = t_i$), the specific activity will thus be:

$$a(t_i) = N\sigma\phi \{1 - \exp(-\lambda t_i)\}, \quad (5.7)$$

so that we see that the specific activity as a function of time is characterized by a buildup from zero to the saturation value of $N\sigma\phi$ for infinitely long irradiations. After the irradiation has ceased ($t > t_i$), the specific activity as a function of the cooling time, t_c , will obviously decay exponentially and be given by:

$$a(t_c) = N\sigma\phi \{1 - \exp(-\lambda t_i)\} \{ \exp(-\lambda t_c) \} \quad (5.8)$$

where t_c is the cooling time; $t_c = t - t_i$. (5.9)

Chapter 5 Induced Radioactivity at Accelerators

For total activities in situations where uniform flux densities of particles of constant energy are incident on a homogeneous "target", one can simply multiply by the volume of the "target"; or in more complex cases involving non-uniform flux densities, one can integrate the above over the volume of the target.

For γ -ray emitters typical of those emitted by accelerator-produced radionuclides in the range of from about 100 keV to 10 MeV, many texts in health physics demonstrate that the absorbed dose rate, dD/dt (rad/h), at a distance r (meters) from a "point" source is given in terms of the source strength, S , (Ci), and the photon energy, E_γ (MeV) by:

$$\frac{dD}{dt} = 0.4 \frac{S}{r^2} \sum_i E_{\gamma i} . \quad (5.10)$$

The summation is over all γ -rays present, including appropriate branching fractions if more than one photon is emitted per decay. If dD/dt is desired as an approximate absorbed dose rate in Gy/h at a distance, r (meters), from a source strength S in GBq, 10^9 Bq, is a better unit of activity than is Bq for practical work, the constant 0.4 becomes 1.08×10^{-4} . One can use the above to determine the absorbed dose rate from a given activated object if it is a point source. For non-point sources, an appropriate spatial integration must be performed.

II. Activation of Accelerator Components

Proton accelerators whose energy exceeds about 10 MeV will produce radioactivity. This will also occur for accelerators of other ions above a specific energy of about 10 MeV/amu. In some special cases radioactivity can be produced at much lower energies because of exothermic nuclear reactions that either produce radionuclides directly or emit neutrons capable of inducing radioactivity through their secondary interactions. If a given accelerator is properly designed with respect to the shielding against prompt radiation and has proper access controls to avoid direct beam-on exposure to people, the induced radioactivity is very likely to be the dominant source of occupational radiation exposure. The experience at most accelerators bears this out in that the vast majority of the radiation exposure incurred by the workers is due to maintenance activities on radioactivated components, handling and moving of activated items, radiation surveys, and radioactive waste handling. An understanding of the production of radionuclides can help reduce personnel exposures through the selection of more appropriate machine component materials and the optimization of decay ("cool-down") times recommended after the beam has been turned off. The primary focus of this section is on proton accelerators because the activation is much more severe at such machines. The treatise by Barbier (Ba69) has rather adequately handled activation by all types of particles.

Chapter 5 Induced Radioactivity at Accelerators

For the lower incident energies (< 30 MeV), one is first concerned with production of radionuclides by such processes as (p, γ) and single- and multi-nucleon transfer reactions. While the details of the total cross sections for such reactions continue to form an interesting subfield of nuclear physics, the systematics and approximate energy dependencies are globally well understood. In general, one is dealing with endothermic nuclear reactions that have a threshold, E_{th} , below which the process is forbidden by conservation of energy. For nuclear reactions induced by ions, E_{th} is related to the reaction Q -value (see Chapter 1), Q_v , by :

$$E_{th} = \frac{m + M}{M} |Q_v|, \quad (5.11)$$

where Q_v is negative in an endothermic reaction having a positive value of E_{th} . In this equation, m is the mass of the incident projectile while M is the mass of the target atom, assumed to stationary in the Laboratory frame of reference. Thick target yields of radionuclides for targets having a range of atomic numbers have been systematically studied by Cohen for a number of nuclear processes spanning the periodic table (Co78). Fig. 5.1 is a representative plot of the general features of such excitation functions of such nuclear reactions. Specific processes may vary considerably from this behavior since “resonances” at specific nuclear excited states have been ignored. Table 5.1 lists a variety of such nuclear reactions along with the range of values of energy above threshold at which the radioactivity production rate has risen to 0.1% of the saturation value and also the range of saturation values for the production of radioactivity. It is assumed that the target thickness comfortably exceeds the range of the incident ion and that the irradiation period greatly exceeds the half-life of the radionuclide of interest. If shorter bombarding periods, t_i , are used, one can correct by multiplying the value by the factor $[1 - \exp(-\lambda t_i)]$. Over the energy range of these curves, the importance of activation by secondary particles is small compared to that encountered at higher energies.

For particle accelerators of higher energy, the neglect of secondary reactions and the restriction to few- and multi-nucleon transfer reactions can become a serious deficiency in the accuracy of estimation of induced radioactivity because of the rise in importance of such processes as spallation. At 40 MeV, only few-nucleon transfer reactions are available while at GeV energies, generally the entire periodic table of nuclides having mass numbers less than that of the target material becomes available. The variety of radionuclides that can be produced increases as one increases the bombarding energy because more thresholds are exceeded. As a general rule, at high energies ($E_0 \approx 1$ GeV or greater), one must consider that all radionuclides in the periodic table which have mass numbers less than that of the material exposed to the flux of hadrons may be produced. Of course, many of these are of little significance due to short lifetimes and small production cross sections. In fact, the production cross sections for specific radionuclides often are nearly independent of the target element.

Chapter 5 Induced Radioactivity at Accelerators

Table 5.2 gives a list radionuclides typically encountered in accelerator installations and their half-lives. In this table only nuclides with half-lives between 10 minutes and 5 years are listed. Also, all "pure" β^\pm emitters are ignored. These are those for which no γ -ray is emitted. Approximate thresholds and high energy cross sections, usually taken from the treatise by Barbier (Ba69) are also provided where available.

A systematic way of handling the great multiplicity of radionuclides produced in accelerator components by high energy particles is highly desirable since it is often not practical to handle them all separately. Global properties of the distribution of radionuclides must be used. Sullivan and Overton (Su65) have treated this problem in an elegant manner that is restated here. The initial starting point is a modification of Eq. (5.8) describing the dose rate as a function of irradiation and cooling times, t_i , and t_c , respectively:

$$\delta(t_i, t_c) = G\phi[1 - \exp(-\lambda t_i)]\exp(-\lambda t_c), \quad (5.12)$$

where $\delta(t_i, t_c)$ is the absorbed dose rate, ϕ is the flux density, and G is a collection of many contributing factors including the production cross section, the energy of the beam, the types of secondary particles produced, the isotopic composition of the irradiated component, the geometry, the energy of the γ -rays produced, and the attenuation coefficients for the γ -rays produced.

If the number of radionuclides produced by the irradiation which have decay constants in the interval between λ and $\lambda + d\lambda$ is represented by the differential, dm , then the corresponding increment in absorbed dose rate, $d\delta(t_i, t_c)$, is given by:

$$d\delta(t_i, t_c) = G\phi[1 - \exp(-\lambda t_i)]\exp(-\lambda t_c)dm. \quad (5.13)$$

If it is assumed that the value of G is independent of λ , or its dependence on λ is small compared to other factors, then one can integrate²:

$$\delta(t_i, t_c) = G\phi \int_{\lambda_0}^{\infty} d\lambda \frac{dm}{d\lambda} [1 - \exp(-\lambda t_i)] \exp(-\lambda t_c). \quad (5.14)$$

²This implicitly makes the assumption that, on average, the cross sections that produce the radionuclides of concern are independent of both the half-lives and the particle energies. Somewhat remarkably, this approximation is sufficiently accurate.

Chapter 5 Induced Radioactivity at Accelerators

Here, λ_0 is the shortest decay constant (longest mean-life) to be considered. Fig 5.2 is a plot of the number of radionuclides as a function of half-life, $t_{1/2}$, that have half-lives less than that particular half-life for several choices of atomic mass number, A . This corresponds to the distribution of radionuclides that could be produced in a target of mass number A irradiated by high energy hadrons. As one can see, these cumulative distributions are well-described for values of half-life between 10^{-3} and 10^3 days by a function of the following form:

$$N(t_{1/2}) = a + b \ln(t_{1/2}), \quad (5.15)$$

where $N(t_{1/2})$ is the number of radionuclides with half-lives less than the value of $t_{1/2}$ and a and b are fitting parameters. Because of the one-to-one correspondence between values of $t_{1/2}$, τ , and λ , one can just as well write

$$m(\lambda) = a + b \ln \lambda, \quad (5.16)$$

where $m(\lambda)$ is the number of radionuclides with decay constants greater than λ for the material of concern. Thus,

$$\frac{dm(\lambda)}{d\lambda} = \frac{b}{\lambda}. \quad (5.17)$$

Substituting into Eq. (5.14), one gets:

$$\begin{aligned} \delta(t_i, t_c) = Gb\phi \int_{\lambda_0}^{\infty} \frac{d\lambda}{\lambda} [1 - \exp(-\lambda t_i)] \exp(-\lambda t_c) = \\ Gb\phi \left\{ \int_{\lambda_0}^{\infty} \frac{d\lambda}{\lambda} \exp(-\lambda t_c) - \int_{\lambda_0}^{\infty} \frac{d\lambda}{\lambda} \exp[-\lambda(t_i + t_c)] \right\}. \end{aligned} \quad (5.18)$$

The changes of variables $\alpha = \lambda t_c$ (first term) and $\alpha' = \lambda(t_i + t_c)$ are helpful;

$$\delta(t_i, t_c) = Gb\phi \left\{ \int_{\lambda_0 t_c}^{\infty} d\alpha \frac{e^{-\alpha}}{\alpha} - \int_{\lambda_0(t_i + t_c)}^{\infty} d\alpha' \frac{e^{-\alpha'}}{\alpha'} \right\}. \quad (5.19)$$

Recognizing that the integrands are identical and simplifying by rearranging the limits of integration, we have

$$\delta(t_i, t_c) = Gb\phi \int_{\lambda_0 t_c}^{\lambda_0(t_i + t_c)} d\alpha \frac{e^{-\alpha}}{\alpha}. \quad (5.20)$$

Chapter 5 Induced Radioactivity at Accelerators

The integral is of a form that integrates to a series expansion found in standard tables of integrals;

$$\int_{x_1}^{x_2} \frac{e^{ax} dx}{x} = \left[\ln x + \frac{ax}{1!} + \frac{a^2 x^2}{2 \cdot 2!} + \frac{a^3 x^3}{3 \cdot 3!} + \dots \right]_{x_1}^{x_2} \quad (5.21)$$

Substituting,

$$\int_{\lambda_0 t_c}^{\lambda_0(t_i+t_c)} \frac{e^{-\alpha} d\alpha}{\alpha} = \left[\ln \alpha - \alpha + \frac{\alpha^2}{4} - \frac{\alpha^3}{18} + \dots \right]_{\lambda_0 t_c}^{\lambda_0(t_i+t_c)} \quad (5.22)$$

Evaluating, one obtains

$$\delta(t_i, t_c) = Gb\phi \left[\ln \left(\frac{t_i + t_c}{t_c} \right) - \lambda_0 t_i + \dots \right] \quad (5.23)$$

Since λ_0 approaches zero (corresponding to large lifetimes), the following is obtained:

$$\delta(t_i, t_c) = B\phi \ln \left(\frac{t_i + t_c}{t_c} \right), \quad (5.24)$$

where several constants are merged in the new parameter B .

Gollon (Go76) has further elaborated on these principles and determined some very useful "rules of thumb" for high energy hadron accelerators at which the extranuclear hadron cascade process produces the major fraction of the induced activity. Four rules are extremely useful for approximate radioactivity estimates:

Rule 1 This is equivalent to Eq. (5.10), restated here for convenience:

$$\frac{dD}{dt} = 0.4 \frac{S}{r^2} \sum_i E_{\gamma i} \quad (5.25)$$

where the summation is over all γ -rays present, including appropriate branching fractions if more than one photon is emitted per decay. If dD/dt is desired as an approximate absorbed dose rate in Gy/h at a distance r (meters) from a source strength S in GBq, the factor 0.4 becomes 1.08×10^{-4} .

Rule 2: In many common materials, about 50 % of the nuclear interactions produce a nuclide with a half-life longer than a few minutes. Further, about 50 % of these have a half-life longer than one day. Thus approximately 25 % of the nuclear interactions (e.g., the "stars" discussed in Chapter 3) produce a radionuclide having a half-life exceeding approximately one day.

Chapter 5 Induced Radioactivity at Accelerators

Rule 3: For most common shielding materials, the approximate dose rate dD/dt due to a constant irradiation is given in Eq. (5.24):

$$\frac{dD}{dt} = B\phi \ln\left(\frac{t_i + t_c}{t_c}\right). \quad (5.26)$$

In the above, the geometry and material dependent factor B can often be determined empirically, or by using rule 2, while ϕ is the incident flux density. This expression appears to be valid also for heavy ion beams at 86 MeV/nucleon according to Tuyn (Tu84).

Rule 4: In a hadronic cascade, a proton produces about four inelastic interactions for each GeV of energy.

These rules can be illustrated by examples. In a short target of 1/10 of an interaction length long, approximately 10 % of an incident beam of 10^{11} protons s^{-1} will interact. Assume this has been occurring for several months (long enough to reach saturation production for many radionuclides). Using Rule 2 in conjunction with the above rate, one determines that the decay rate after one day of the shutdown is 2.5×10^9 Bq (68 mCi). If each of these decays produces a one MeV γ -ray, then Rule 1 will indicate an absorbed dose rate of 27 mrad/h (≈ 0.27 mGy/h of absorbed dose rate) at one meter away.

Rule 3 can be used in such a calculation to predict the absorbed dose rate from a point source at some future time after beam shutdown. Furthermore, this rule is not restricted to "point" sources but can be used for more massive ones, with suitable adjustments to the geometry factors. Sometimes one can estimate the product $B\phi$ or use a measurement of the exposure or absorbed dose rate to determine it empirically for the purpose of using Eq. (5.26) to predict the "cooldown". In this way, Rule 3 is also useful for extended shields irradiated by secondary particles from a well-developed cascade. Rule 4 can be used to crudely estimate the activation of a beam dump by incident high energy particles when it is coupled with Rule 2.

Rule 4 can be used thus: A beam of 10^{12} 400 GeV p/s ($= 0.16 \mu\text{A}$ or 64 kW) produces a total of $4 \times 400 \times 10^{12}$ stars/s in a beam dump. If 25 % of these produce a radionuclide with a half-life > 1 day (Rule 2), then the total amount of the moderately long-lived radioactivity (at saturation) is:

$$\frac{(0.25 \text{ atoms/star})(1.6 \times 10^{15} \text{ stars/sec})}{3.7 \times 10^{10} \text{ sec}^{-1} \text{ Ci}^{-1}} = 10.8 \text{ kCi} . \quad (5.27)$$

At sufficiently large distance (say 10 meters), Rule 1 could be used to calculate an absorbed dose rate assuming all decays are 1 MeV γ -rays:

$$\frac{dD}{dt} = 0.4(1 \text{ MeV}) \left(\frac{1.08 \times 10^4 \text{ Curies}}{10^2 \text{ meter}^2} \right) = 43 \text{ rads / hour} . \quad (5.28)$$

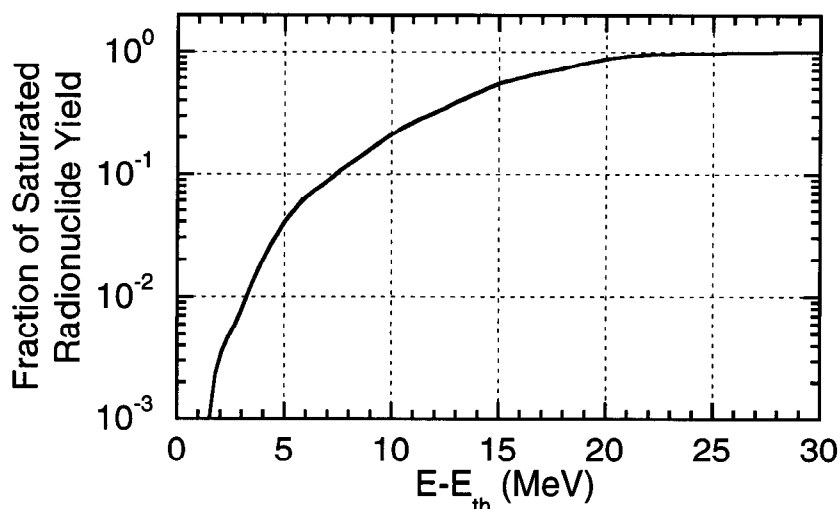


Fig. 5.1 Typical behavior of radionuclide production by (p, γ) or few-nucleon transfer reactions for energies not far above the reaction threshold, E_{th} . This behavior is typical of the nuclear reactions tabulated in Table 5.1. For detailed calculations, data related to specific reactions on specific target materials should be used. [Adapted from Co78].]

Table 5.1 Tabulation of generalized parameters for the production of radionuclides by means of low energy nuclear reactions which span the periodic table. The ranges of energies are listed at which the production yields are at approximately one per cent of the tabulated saturation values. The "high/low" values for the saturated activity are also given. [Adapted from (Co78).]

Reaction	0.1% Yield-low (E-E _{th}) (MeV)	0.1% Yield-high (E-E _{th}) (MeV)	Sat. Yield-low (μ Ci/ μ A)	Sat. Yield-high (μ Ci/ μ A)	Reaction	0.1% Yield-low (E-E _{th}) (MeV)	0.1% Yield-high (E-E _{th}) (MeV)	Sat. Yield-low (μ Ci/ μ A)	Sat. Yield-high (μ Ci/ μ A)
(p, γ)	4	9	3×10^2	10^3	(3 He, γ)	4	6	1	2
(p,n)	0	6	3×10^5	8×10^5	(3 He,n)	3	12	10^2	3×10^2
(p,2n)	1	4	3×10^5	10^6	(3 He,2n)	2	7	3×10^2	4×10^3
(p,3n)	1	6	3×10^5	10^6	(3 He,3n)	2	5	2×10^3	3×10^4
(p,4n)	5	8	2×10^5	10^6	(3 He,2p)	4	12	2×10^2	10^4
(p,5n)	5	10	10^5	2×10^6	(3 He, α)	6	14	2×10^2	10^3
(p,pn)	2	5	2×10^5	2×10^6	(3 He,p3n)	10	15	10^4	4×10^5
(p,p2n)	3	8	3×10^5	2×10^6	(α , γ)	10	13	3	20
(d, γ)	5	7	30	100	(α ,n)	1	9	3×10^2	10^4
(d,n)	2	7	4×10^3	3×10^5	(α ,2n)	1	4	5×10^3	4×10^4
(d,2n)	2	5	2×10^5	6×10^6	(α ,3n)	1	6	3×10^3	7×10^5
(d,3n)	1	4	3×10^5	10^6	(α ,4n)	5	8	3×10^3	4×10^4
(d,4n)	4	8	2×10^5	6×10^5	(α ,5n)	5	8	10^4	3×10^5
(d,5n)	6	10	10^5	10^6	(α ,p)	5	8	6×10^2	2×10^4
(d,p)	2	7	4×10^4	3×10^5	(α ,pn)	3	12	3×10^3	8×10^4
(d,p2n)	2	10	10^5	2×10^6	(α ,p2n)	5	15	3×10^3	7×10^4
(d,p3n)	8	15	10^5	2×10^6	(α ,p3n)	7	15	10^4	3×10^4
(d,2p)	5	15	3×10^3	4×10^4	(α ,2p)	5	10	10^2	3×10^3
(d, α)	4	7	10^4	3×10^4	(α , α n)	6	16	3×10^3	3×10^4
(d, α n)	5	15	2×10^4	10^5					

Chapter 5 Induced Radioactivity at Accelerators

Table 5.2 Summary of radionuclides commonly identified in materials irradiated around accelerators. Approximate cross sections for their production at the high energy limit and approximate thresholds are given for selected radionuclides.

[Adapted from (NC99) and (Ba69).]

Target Material	Radionuclides	Approximate Threshold (MeV)	Half-life	Production Cross Section (High Energy Limit) (mb)
Plastics & Oils	^3H	11	12.33 years	10
	^7Be	2	53.6 days	10
	^{11}C	20	20.4 minutes	20
Aluminum, Concrete	As above, plus			
	^{18}F	40	109.7 minutes	6
	^{22}Na	30	2.6 years	10
	^{24}Na	5	15.0 hours	10
	As above, plus			
Iron	^{42}K		12.47 hours	
	^{43}K		22.4 hours	
	^{44}Sc		3.92 hours	
	$^{44\text{m}}\text{Sc}$		2.44 days	
	^{46}Sc		84 days	
	^{47}Sc		3.43 days	
	^{48}Sc		1.83 days	
	^{48}V	20	16.0 days	6
	^{51}Cr	30	27.8 days	30
	^{52}Mn	20	5.55 days	30
	$^{52\text{m}}\text{Mn}$		21.3 minutes	
	^{54}Mn	30	300 days	30
	^{52}Fe	30	8.3 hours	4
	^{55}Fe		2.94 years	
	^{59}Fe		45.1 days	
	^{56}Co	5	77 days	30
	^{57}Co	30	270 days	30
^{58}Co	30	72 days	25	
Copper	As above, plus			
	^{57}Ni	40	37 hours	2
	^{65}Ni		2.56 hours	
	^{60}Co	30	5.27 years	15
	^{60}Cu		23 minutes	
	^{61}Cu	20	3.33 hours	100
	^{62}Cu		9.80 minutes	
	^{64}Cu		12.82 hours	
	^{62}Zn	15	9.13 hours	60
	^{65}Zn	0	244 days	100

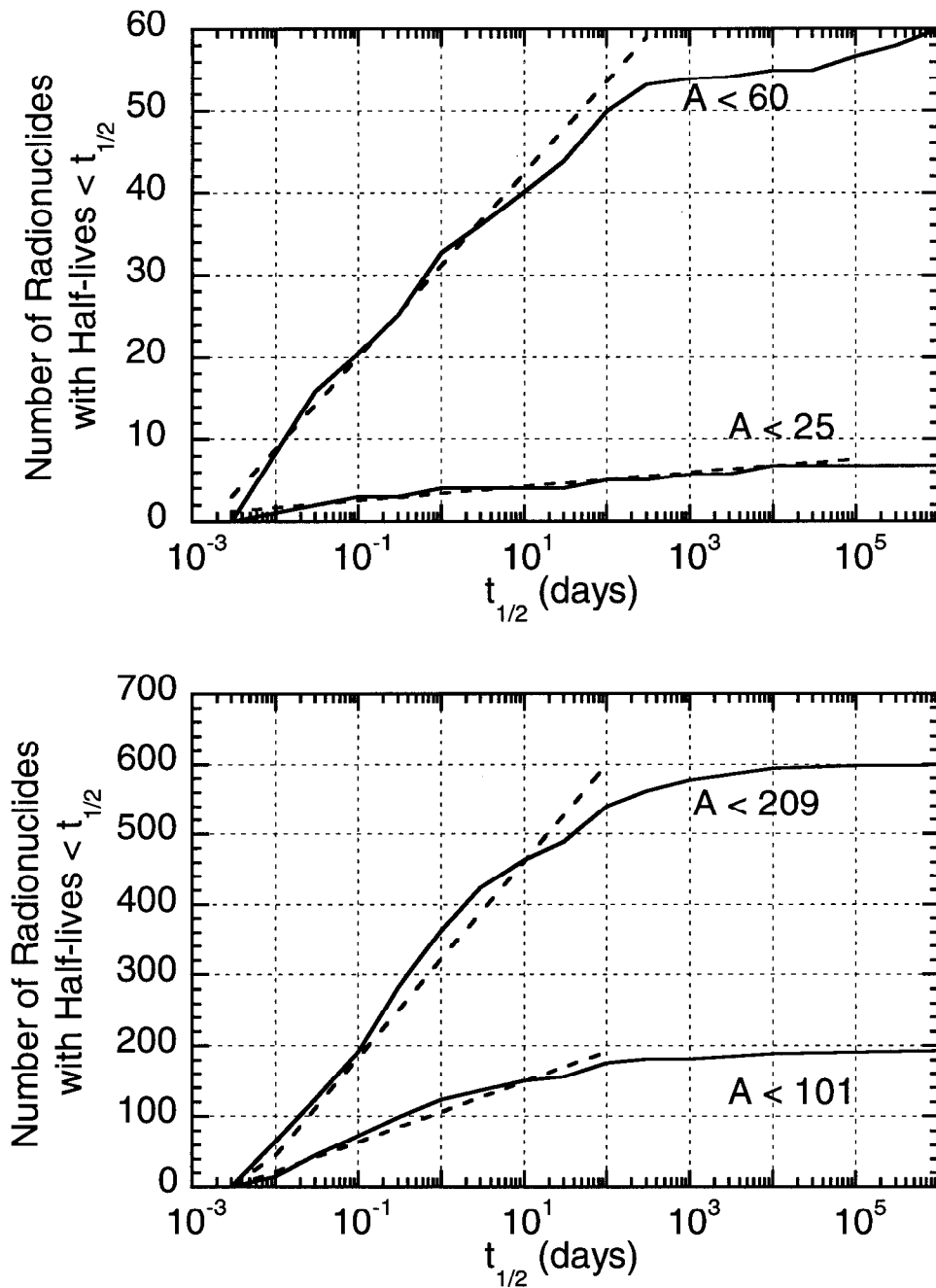


Fig. 5.2 Total number of radionuclides having half lives up to a given half-life as a function of half-life for target mass numbers less than those indicated. [Adapted from (Ba69).]

Chapter 5 Induced Radioactivity at Accelerators

A valuable quantity used to quantify the absorbed dose rate, dD/dt , at the surface of a thick target is the **danger parameter, D** , as developed by Barbier (Ba69) for a thick object irradiated by beam having a uniform flux density ϕ . If this source of radioactivity subtends solid angle Ω at the point of concern, then

$$\frac{dD}{dt} = \frac{\Omega}{4\pi} \phi D. \quad (5.29)$$

For contact with a semi-infinite slab of uniformly irradiated material, the fractional solid angle factor ($\Omega/4\pi$) has the intuitively obvious value of 1/2. The danger parameter has the physical interpretation as the absorbed dose rate found inside a cavity of arbitrary form embedded in an infinite volume of a material which has been uniformly irradiated by a unit flux density (one particle per second per square centimeter). Figures 5.3 give representative examples of plots of D for several elements and a few compounds. These curves thus can be used to predict cooling of various components around accelerators. Gollon (Go76) has also provided "cooling curves" for iron struck by high energy protons. These are given in Fig. 5.4 and include both calculations by Armstrong and Alsmiller (Ar73) and empirical measurements at the Brookhaven National Laboratory AGS, the Fermilab Main Ring Accelerator, and the Fermilab Neutrino Experimental Area target station.

Of course, one is often concerned with situations where the determination of ϕ in the danger parameter equation is not at all simple. For example, one can have activation in a large object where the hadronic cascade is contributing numerous hadrons at a variety of energies from a multitude of directions. Fortunately, important features of activation phenomena have little or no correlation with energy. The chief of these is evidenced by the excitation functions of various reactions. In general, the cross sections rise just above the threshold and then, somewhere in the region of 10's of MeV, a leveling-off occurs. Furthermore, in general the cross sections for production of radionuclides by neutrons and protons (and even other ions and particles) do not differ from each other at the higher energies.

The "leveling-off" of the cross section has some very important implications the most important is the fact that for estimating activation, one can perform approximate calculations without performing an integration over energy if one has some reasonable estimate of the flux above the reaction threshold of interest. An average effective cross section can then be used. The leveling off also renders reasonable the use of threshold detectors in instrumentation as discussed in Chapter 6. Another feature of these excitation functions is the fact that the leveling off occurs in the region from a few 10's to a few 100's of MeV precisely where relatively fast Monte-Carlo hadron shielding calculations are available from several different codes (e.g., CASIM, FLUKA, HETC, and MARS).

Chapter 5 Induced Radioactivity at Accelerators

It is often possible to relate the flux density of high energy hadrons (i.e., those with energies above the leveling off) to the star density, S , calculated from such Monte-Carlo calculations through the relationship,

$$\phi(\vec{r})(\text{cm}^{-2}\text{sec}^{-1}) = \frac{\lambda(\text{g cm}^{-2})}{\rho(\text{g cm}^{-3})} \frac{dS(\vec{r})}{dt} \left(\frac{\text{stars cm}^{-3}}{\text{sec}} \right), \quad (5.30)$$

where $\phi(\vec{r})$, the flux density at position vector \vec{r} , is related to the rate of star density production $\frac{dS(\vec{r})}{dt}$ ($\text{stars cm}^{-3} \text{ s}^{-1}$) at the same location. The density is denoted by ρ and the interaction length is denoted by λ . [In the context of this discussion, care must be taken not to confuse interaction length with activity constant since they are customarily denoted by the same symbol, λ .] The value of $\phi(\vec{r})$ so determined could, in principle, be substituted into the equation given above for calculating absorbed dose rate due to residual activity using the Barbier danger parameter, \mathbf{D} , if one were to make suitable adjustments in the solid angle. However, the limitation of this approach is the fact that the Monte-Carlo cutoffs may introduce an energy (or momentum) cutoff (e.g., typically 300 MeV/c in CASIM) which is not necessarily matched to the reaction threshold. In order to calculate dose equivalent rates, Gollon (Go76) made detailed calculations and obtained the following formula:

$$\frac{dD(\vec{r})}{dt} = \frac{\Omega}{4\pi} \frac{dS(\vec{r})}{dt} \omega(t_i, t_c), \quad (5.31)$$

where $\omega(t_i, t_c)$ is related to the Barbier danger parameter, \mathbf{D} . For iron, Gollon gives the following values for two useful situations:

$$\omega(\infty, 0) = 9 \times 10^{-6} \text{ rad h}^{-1}/(\text{star cm}^{-3} \text{ s}^{-1}) \quad (5.32a)$$

(infinite irradiation, zero cooling time) and

$$\omega(30 \text{ d}, 1 \text{ d}) = 2.5 \times 10^{-6} \text{ rad h}^{-1}/(\text{star cm}^{-3} \text{ s}^{-1}) \quad (5.32b)$$

(30 days irradiation, 1 day cooling time).

Estimates of the ω -values can be made by scaling results obtained by Armstrong and Alsmiller (Ar69a) and Gabriel and Santoro (Ga73) for selected values of t_i and t_c . This has been done by Cossairt (Co98) for three choices of values of t_i , and the results are shown in Fig. 5.5. Gollon derived a simple relationship between dose rates involving cooling times different from "standard" ones for which values of \mathbf{D} and ω are available. As stated previously, the dose rate after irradiation time t_i and cooldown time t_c is

$$\delta(t_i, t_c) = \sum_{\mu} A_{\mu} \left[1 - \exp(-\lambda_{\mu} t_i) \right] \exp(-\lambda_{\mu} t_c), \quad (5.33)$$

where the summation over index μ includes all relevant radionuclides with the product of flux density and geometry factors being absorbed (and allowed to vary with radionuclide) in the quantity A_{μ} .

Chapter 5 Induced Radioactivity at Accelerators

Rearranging, Gollon obtained:

$$\delta(t_i, t_c) = \sum_{\mu} A_{\mu} \left[\exp\{-\lambda_{\mu} t_c\} - \exp\{-\lambda_{\mu}(t_i + t_c)\} \right] = \delta(\infty, t_c) - \delta(\infty, t_i + t_c). \quad (5.34)$$

Thus, the infinite irradiation curve can be used to determine any other combination of the times t_i and t_c . In fact, this formula may be used also with empirical results such as, for example, radiation survey data, in order to predict future radiological conditions.

A reliable method for connecting the production of "stars" in material (e.g., as calculated by a Monte-Carlo code) to the production of atoms of some radionuclide is by the ratios of cross sections. Thus, at some point in space, \vec{r} , the rate of production of atoms per cm^3 , $n(\vec{r})$, of some radionuclide is approximately given by:

$$\frac{dn(\vec{r})}{dt} \approx \frac{\sigma_r}{\sigma_{in}} \frac{dS(\vec{r})}{dt} = \frac{\Sigma_r}{\Sigma_{in}} \frac{dS(\vec{r})}{dt}, \quad (5.35)$$

where one essentially scales the star density production rate [e.g., stars/(cm^3 -s)] by the ratio of the production (reaction) cross section for the nuclide of interest, σ_r , to the total inelastic cross section σ_{in} or, equivalently, by the macroscopic cross section ratio (Σ_r/Σ_{in}). At saturation after a long irradiation, this will be the rate of decay as well. The phenomena will obey the usual activation equation. The reason this is approximate is due to the standard concerns about constancy of cross sections with energy, the lack of perfect "matching" of thresholds, etc.

Somewhat special considerations may apply to the concrete shielding surrounding accelerators. As was seen before, ordinary concrete typically contains a partial density of 0.04 g/ cm^3 of Na. This "typical" value varies a great deal due to the variety of minerals which might be present in local concrete. The significance of this seemingly small additive is that the naturally dominant isotope present is ^{23}Na . This nucleus has the relatively large thermal neutron capture cross section of 535 mb.

Patterson (Pa58) determined that average thermal flux density, ϕ_{th} , in a concrete room is approximately given as follows:

$$\phi_{th} = \frac{1.25Q}{S}, \quad (5.36)$$

where Q is the number of fast neutrons produced per second in the enclosure and S is the inside surface area of the enclosure (cm^2). Thus, a substantial flux density of thermal neutrons can be present in an accelerator room and this flux can produce significant amount of ^{24}Na with its 15 hour half-life. The relatively high energy photon emitted in its decay (2.75 MeV) also can enhance the radiation hazard. Furthermore, while the dose due to activated components falls off radially with distance, if absorption by the air is not

Chapter 5 Induced Radioactivity at Accelerators

significant, the absorbed dose rate due to residual activation in an empty cylindrical room uniformly irradiated by such thermal neutrons is a constant. Thus, the dose equivalent rate anywhere inside the enclosure will be equal to the dose equivalent at the wall. This has been explicitly demonstrated for cylinders by Armstrong and Barish (Ar69b) and is also true for the interior of all mathematically well-behaved closed surfaces (Co96). This fact can readily be demonstrated by analogy to the Gauss Law in electrostatics as follows by examining the situation in Fig. 5.6. Consider a simple, closed surface which emits an omnidirectional flux density of some particle ϕ_0 (e.g., particles $\text{cm}^{-2}\text{s}^{-1}$) that is constant over the surface. One wants to calculate the flux density at some point in space P within the surface. P is located at radius vector \vec{r} . Consider, further, the contributions of the particle emitted by some elemental area $d\vec{A}$ at P where $d\vec{A}$ is perpendicular to the surface at coordinate vector \vec{r}' . The solid angle subtended at P by $d\vec{A}$ is;

$$d\Omega = \frac{d\vec{A} \cdot \hat{n}}{|\vec{r}' - \vec{r}|^2} \quad (5.37)$$

where the unit vector \hat{n} is given by

$$\hat{n} = \frac{\vec{r}' - \vec{r}}{|\vec{r}' - \vec{r}|} \quad (5.38)$$

But the increment of flux at point P due to elemental area $d\vec{A}$ is given by:

$$d\phi = \frac{\phi_0}{4\pi} \frac{d\vec{A} \cdot \hat{n}}{|\vec{r}' - \vec{r}|^2}.$$

Thus,

$$d\phi = \frac{\phi_0}{4\pi} d\Omega \quad \text{and} \quad \phi = \oint_{4\pi} \frac{\phi_0}{4\pi} d\Omega = \phi_0. \quad (5.39)$$

In some cases it has been important to minimize the amount of sodium in the concrete ingredients in order to reduce exposures to individuals conducting maintenance on the accelerator. In fact, the phenomena described above has been noticed at accelerators and sometimes leads to "disappointment" in how little gamma-ray exposure rates are reduced when activated accelerator components are removed from enclosures with equally activated walls. For example, Armstrong and Barish (Ar69b) have calculated residual dose rates inside a cylindrical accelerator tunnel due to both the magnets and the concrete walls for 3 GeV protons incident on iron. These authors have also considered some other reactions that are capable of also producing ^{24}Na (spallation) which also must be included. The results are shown in Fig. 5.7 for the surface at the tunnel wall.

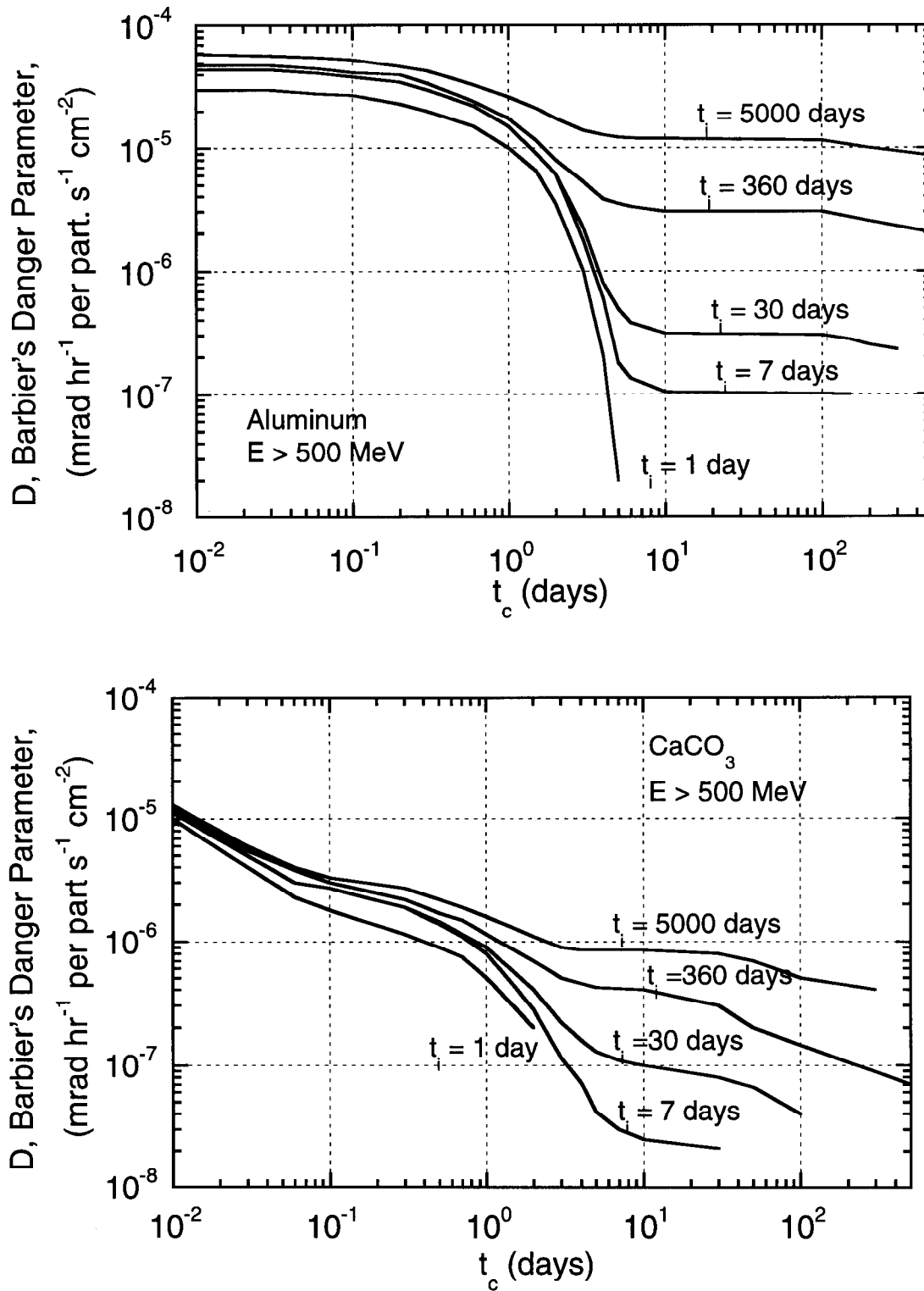


Fig. 5.3 Values of the Barbier danger parameter, D , for selected materials at a proton irradiation energy of 500 MeV. [Adapted from (Ba69).]

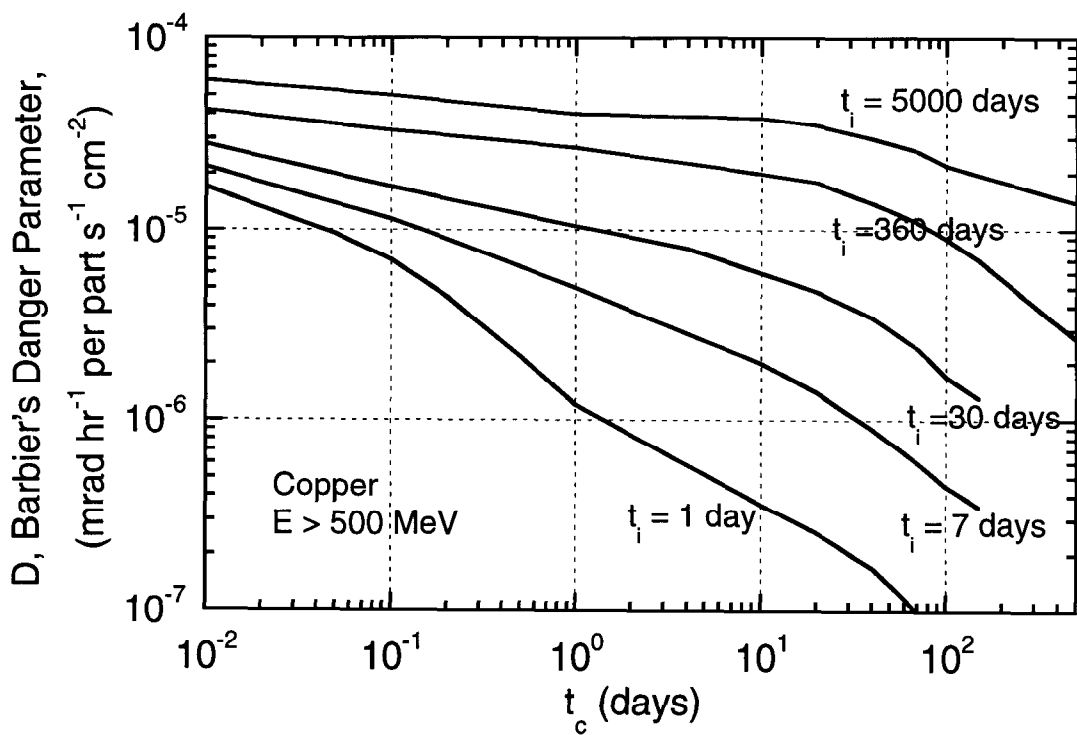
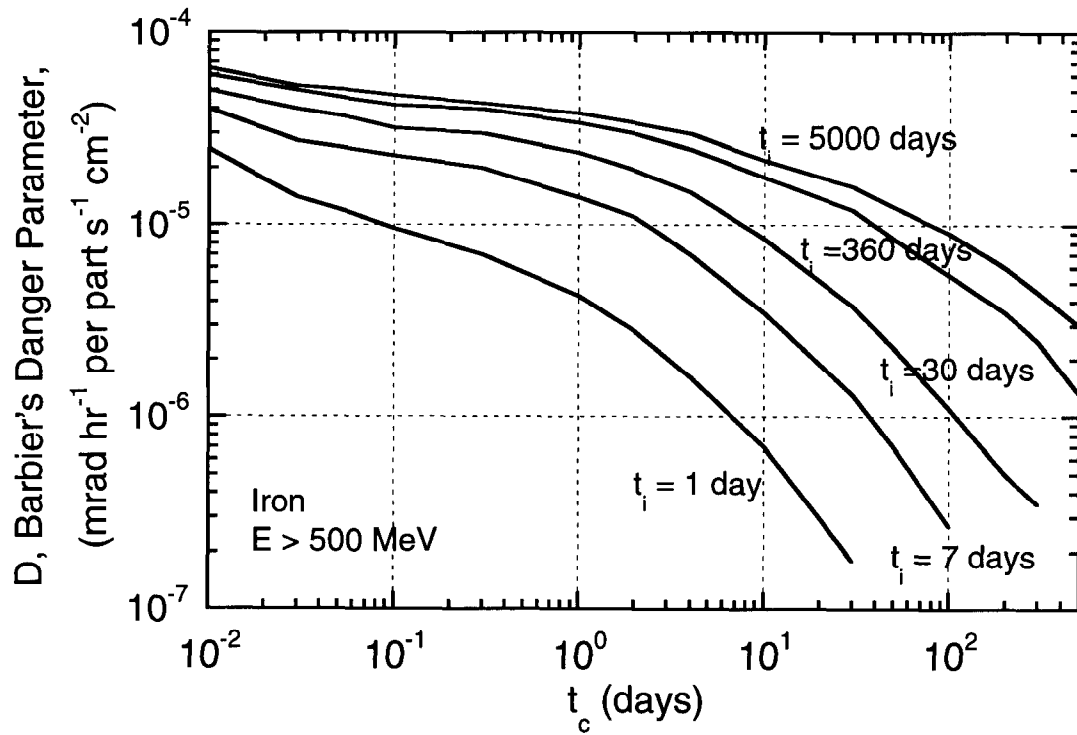


Fig. 5.3-continued.

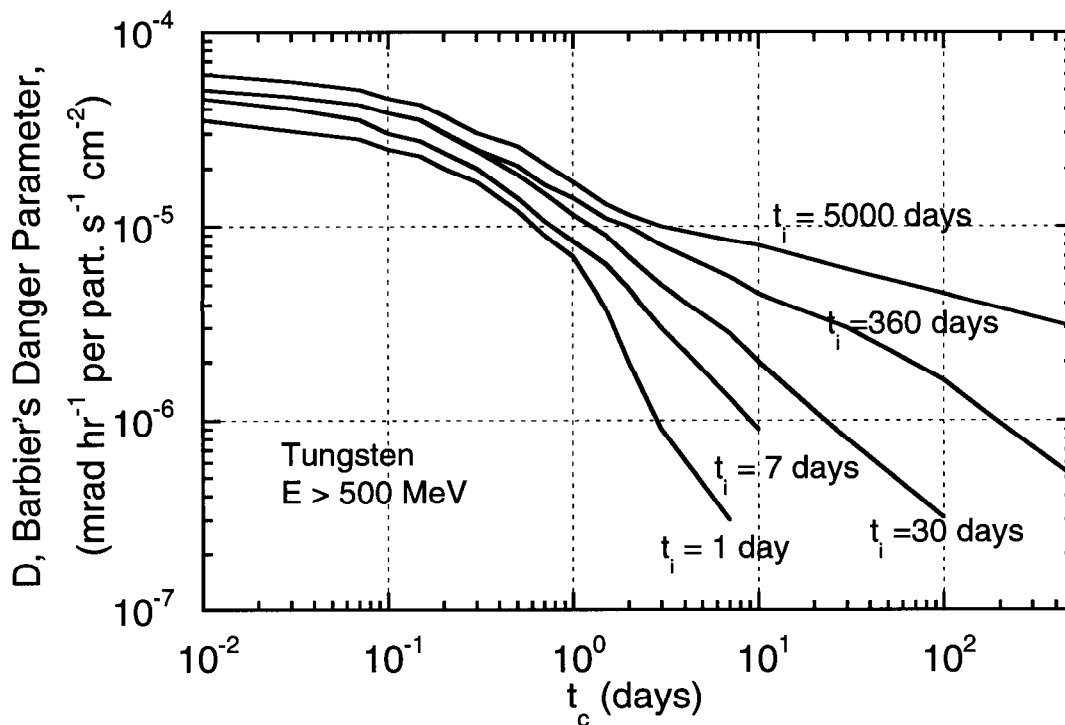


Fig. 5.3-continued.

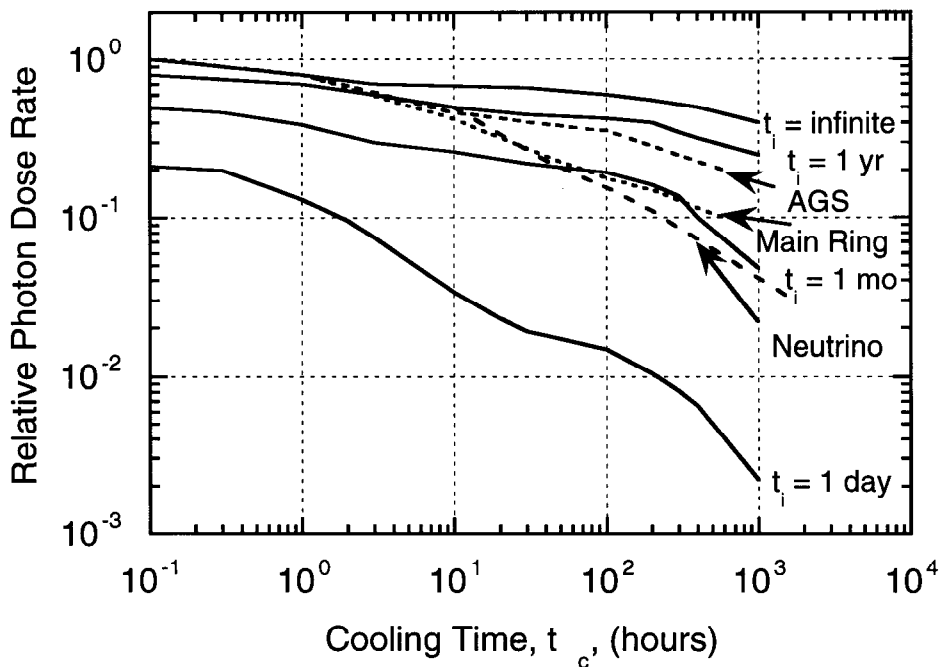


Fig. 5.4 Cooling curves for various irradiation times for iron struck by high energy protons as calculated by Armstrong and Alsmiller (Ar73). Also shown are the results of measurements. The one labeled "Main Ring", is the measured average cooling curve for the Fermilab Main Ring synchrotron after its initial three years of operation. The curve labeled "Neutrino" is for a neutrino target station at Fermilab after eight months of operation. The curve labeled "AGS" is for an extraction splitter in use for many years at the BNL AGS. [Adapted from (Go76).]

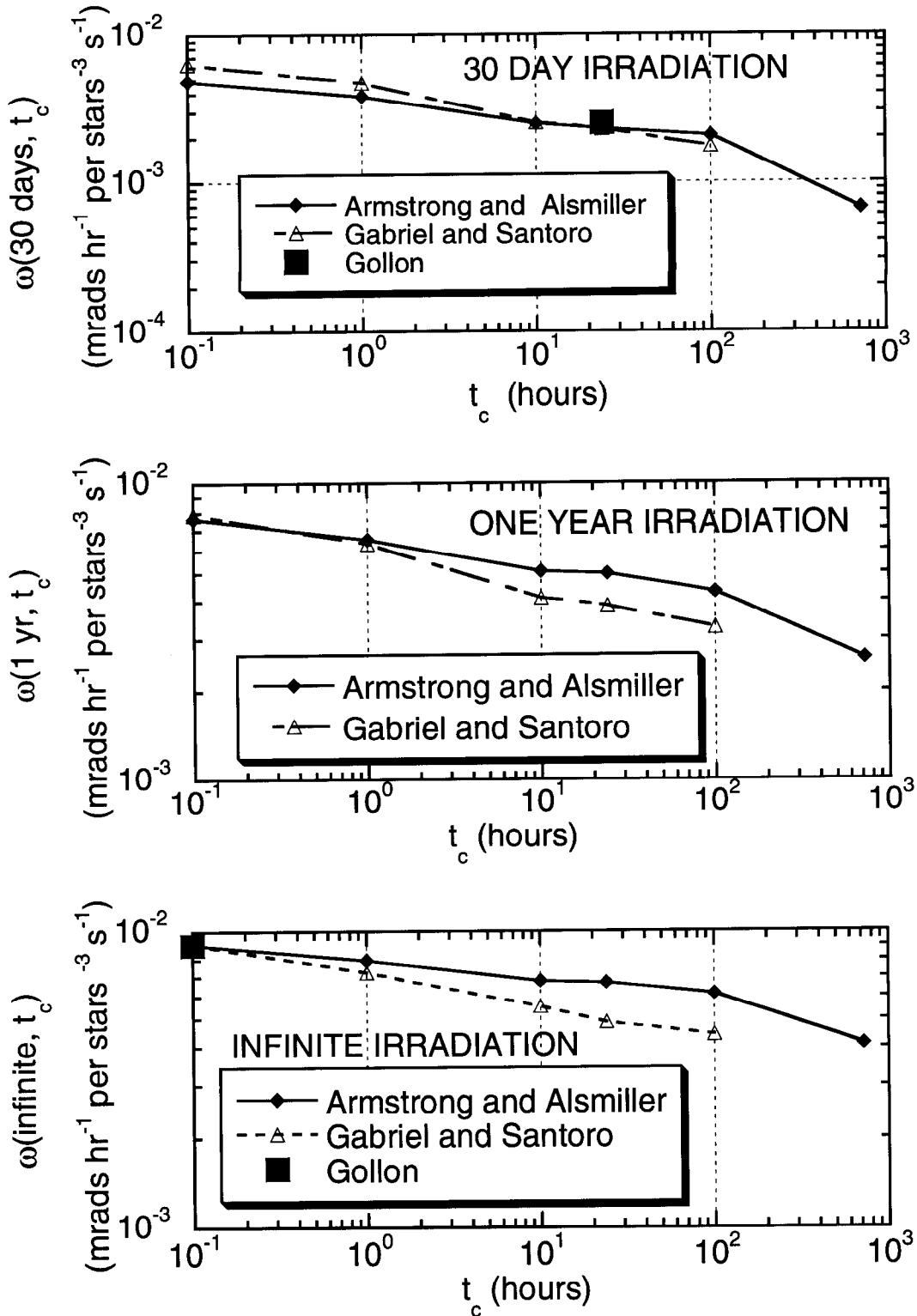


Fig. 5.5 Extrapolations of the cooling factor $\omega(t_i, t_c)$ from the work of Armstrong and Alsmiller (Ar69a) and Gabriel and Santoro (Ga73) compared with those of Gollon (Go76). [Reproduced from (Co96).]

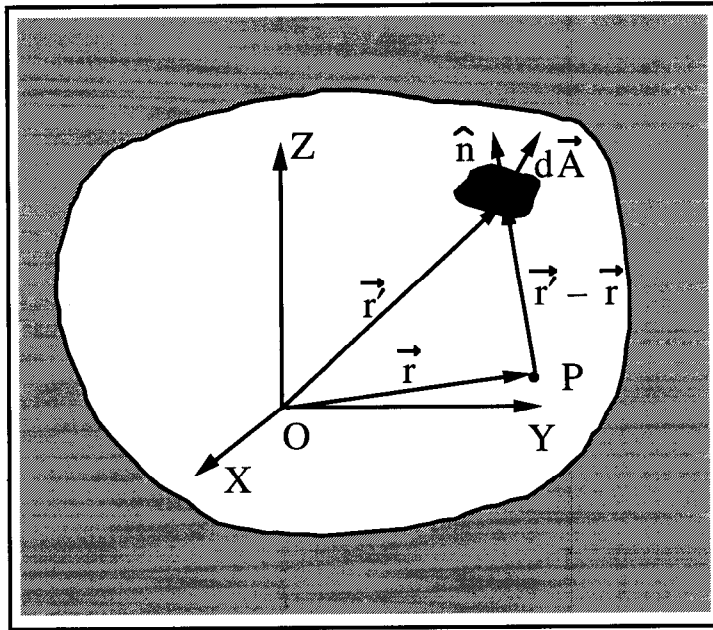


Fig. 5.6 Geometry for deriving relationship between a surface of uniform emission and the flux density at any point within it.

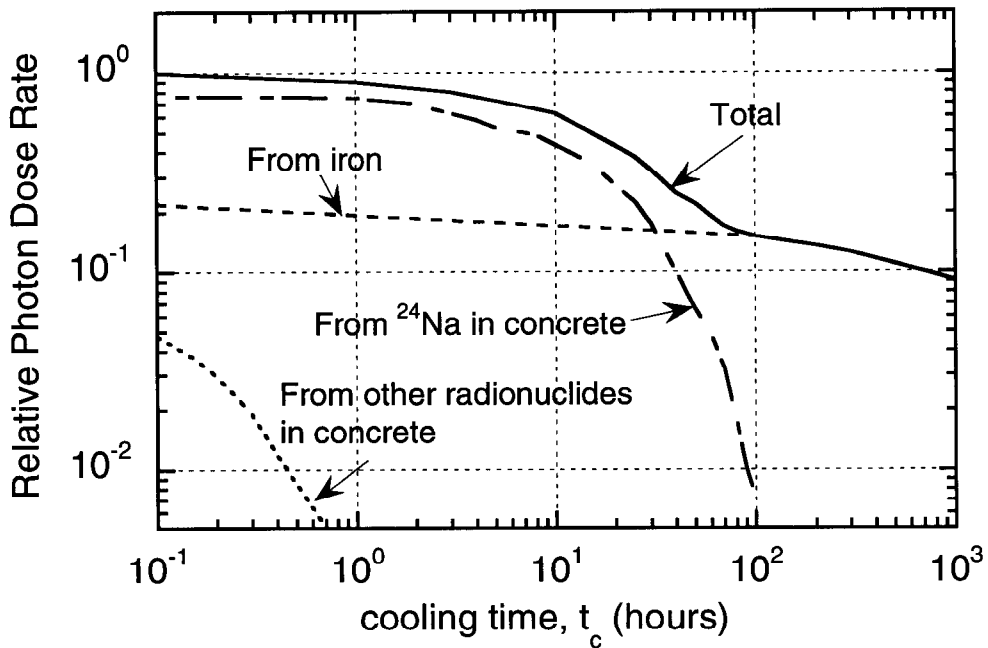


Fig. 5.7 Photon dose rate at surface of tunnel wall after infinite irradiation time for concrete containing one per cent sodium by weight. [Adapted from (Ar69b).]

III. Production and Propagation of Airborne Radioactivity

Production of Airborne Radioactivity

Thomas and Stevenson have presented a very useful synopsis of the production of activity in the atmosphere which is largely followed here (Th88). Some of this same discussion also was presented by Swanson and Thomas (Sw90). The principal source of radioactivity in air at accelerators is due to the interaction of primary and secondary particles directly with the constituent target nuclei in the air in accelerator enclosures. Activated dust and gaseous emission from activated liquids are of secondary importance. Table 5.3 gives the most abundant stable isotopes found in the atmosphere.

Table 5.3 Most abundant stable isotopes in the atmosphere [Adapted from (Th88).]

Isotope	Percentage by volume in the atmosphere
¹⁴ N	78.1
¹⁶ O	21.2
⁴⁰ Ar	0.46
¹⁵ N	0.28
¹⁸ O	0.04

Since low energy accelerators contain their beams in continuous vacuum pipes, the activation of air at these machines is greatly minimized. At high energy accelerators, it is quite common to have air gaps at certain "interface points" and devices associated with beam targetry or beamline diagnostic instrumentation render continuous vacuum impractical. These "air gaps" are only characteristic of extracted beam lines while the accelerator beam chambers are, of necessity, contained in continuous vacuum. In addition, the large multiplicity of secondary particles produced as a part of cascade (both electromagnetic and hadronic) processes can produce airborne radioactivity even where the beams themselves are contained in vacuum.

Table 5.4 lists the radionuclides that can be produced from the principle constituents in air along with the reaction mechanisms associated with their production and an estimate of the average production cross section. The large cross section for neutron induced (n,γ) and (n,p) reactions are for captures of neutrons of thermal energies ($E_n \approx 0.025$ eV) while the remaining cross sections are generally the saturation cross sections found in the region above approximately a few 10's of MeV. The γ-induced reactions are present at virtually all accelerators and most energies.

If the accelerator enclosures were completely sealed, there would be no releases to the outside world and the hazard of these airborne radionuclides would be entirely restricted to those who might have to enter the enclosures. This would, however, allow the longer-lived radionuclides to build up in accord with Eq. (5.8). Also, ventilation is generally needed to provide cooling of components and fresh breathing air for workers. Typically, the "residence time" of air in accelerator enclosures is limited to a range of time between

Chapter 5 Induced Radioactivity at Accelerators

approximately 30 minutes and one hour. Thus, the typical half-lives of the accelerator environment, in equilibrium, will have half-lives only up to the order of one hour. The residence time of the air in conjunction with the cross sections determines the radionuclides of importance.

Table 5.4 Radionuclides with half-life > 1 minute that can be produced in air at accelerators. [Adapted from (Sw90).]

Radionuclide	Half-life	Emission	Parent Element	Production Mechanism	High Energy Cross Section (mb)
³ H	12.3 years	β^-	N	Spallation	30
			O	Spallation	30
⁷ Be	53.3 days	γ , elect. capt.	N	Spallation	10
			O	Spallation	5
			Ar	Spallation	0.6
¹¹ C	20.4 minutes	β^+	N	Spallation	10
			O	Spallation	0.7
			Ar	Spallation	0.7
¹⁴ C	5730 years	β^-	N	(n,p)	1640
¹³ N	9.96 minutes	β^+	N	Spallation	10
			N	(γ ,n)	10
			O	Spallation	9
¹⁴ O	70.6 seconds	β^+ , γ	Ar	Spallation	0.8
			O	Spallation	1
			Ar	Spallation	0.06
¹⁵ O	2.03 minutes	β^+	O	Spallation	40
			O	(γ ,n)	10
			Ar	Spallation	
¹⁸ F	1.83 hours	β^+ , elect. capt.	Ar	Spallation	6
²⁴ Ne	3.4 minutes	β^- , γ	Ar	Spallation	0.12
²² Na	2.6 hours	β^+ , γ	Ar	Spallation	10
²⁴ Na	15.0 hours	β^-	Ar	Spallation	7
²⁷ Mg	9.46 minutes	β^- , γ	Ar	Spallation	2.5
²⁸ Mg	20.9 hours	β^- , γ	Ar	Spallation	0.4
²⁸ Al	2.25 minutes	β^- , γ	Ar	Spallation	13
²⁹ Al	6.6 minutes	β^- , γ	Ar	Spallation	4
³¹ Si	2.62 hours	β^- , γ	Ar	Spallation	6
³⁰ P	2.50 minutes	β^+ , γ	Ar	Spallation	4.4
³² P	14.3 days	β^-	Ar	Spallation	25
³³ P	25.3 days	β^-	Ar	Spallation	9
³⁵ S	87.5 days	β^-	Ar	Spallation	23
^{34m} Cl	32.0 minutes	β^- , γ	Ar	Spallation	0.7
³⁸ Cl	37.2 minutes	β^- , γ	Ar	(γ ,pn)	4
			Ar	(γ ,p)	7
³⁹ Cl	55 minutes	β^- , γ	Ar	(γ ,p)	7
⁴¹ Ar	1.8 hours	β^- , γ	Ar	(n, γ)	660

Chapter 5 Induced Radioactivity at Accelerators

In general, the positron emitters ^{11}C , ^{13}N , ^{15}O along with ^{41}Ar (produced by thermal capture) are the nuclides most frequently seen. Recent work at Fermilab described in by Butala et al. (Bu89) and Vaziri et al. (Va93), and (Va94) has also confirmed these identifications and, additionally, detected ^{39}Cl . At electron accelerators, the copious presence of photons will enhance the photon-induced production processes and hence the production of ^{38}Cl and ^{39}Cl . It should be pointed out that distinguishing between the positron emitters must principally be done by fitting decay curves. This is a result of the fact that their γ -ray spectra are all comprised of 0.511 MeV photons from positron annihilation. Such decay curves have been analyzed (by fitting with sums of exponentials representing the half-lives possible) and used to determine proportions of the various radionuclides in references (Th88), (Sw90), (Bu89), (Va93), and (Va94).

It was concluded by Butala et al. that the geometry of target stations can significantly affect the composition (Bu89). For example, high intensity targets immediately surrounded with large volumes of iron and concrete (in contact with the iron) produced much less ^{41}Ar than did other targets where the bulk iron shield was located in a open room with a layer of air between the iron and the concrete. Presumably, the open space provided opportunity for the large flux of 0.847 MeV neutrons expected external to a pure iron shield (see Chapter 3) to "thermalize" and thus enhance the production of ^{41}Ar in the air space. The large cross section for the $^{40}\text{Ar}(n,\gamma)^{41}\text{Ar}$ reaction at thermal neutron energies ($\sigma_{th} = 660$ mb) also may have provided the photons necessary to enhance the (γ, p) and (γ, pn) reactions required to produce significant quantities of ^{39}Cl and ^{38}Cl , respectively. Some typical percentages of the various radionuclides (by activity concentration) are given in Table 5.5.

Table 5.5 Measured radionuclide composition of typical airborne releases from accelerators

Situation	Radionuclides (Activity Per Cent)					
	^{11}C	^{13}N	^{15}O	^{38}Cl	^{39}Cl	^{41}Ar
CERN (Th88) 28 GeV protons	31.0	47.0	8.0			14.0
Fermilab (Bu89) 800 GeV protons						
(no gap between iron and concrete walls)	46.0	19.0	35.0			
(gap between iron and concrete walls)	42.0	14.0	0.0	0.0	10.0	34.0
Fermilab (Va93) 120 GeV protons	58.5	37.9		1.0	1.1	1.5
Fermilab (Va94) 120 GeV protons	64.6	30.5				5

Patterson and Thomas (Pa73), have used the expanded general activation equation to derive the total specific activity, S (typically in units of Bq/cm^3) of an enclosed volume of radioactive air;

$$S = C \sum_i \left[\sum_j \phi_\gamma N_j \bar{\sigma}_{ij\gamma} + \sum_j \phi_{th} N_j \bar{\sigma}_{ij_{th}} + \sum_j \phi_{HE} N_j \bar{\sigma}_{ij_{HE}} \right] [1 - \exp(-\lambda_i t_i)] \exp(-\lambda_i t_c) \quad (5.40)$$

where ϕ_γ , ϕ_{th} , and ϕ_{HE} , represent the average photon, thermal neutron and high energy flux densities. As before, in this equation t_i is the irradiation time while t_c represents

Chapter 5 Induced Radioactivity at Accelerators

the decay time. The $\bar{\sigma}_{ij}$ values are the corresponding cross sections averaged with the energy-dependent flux density over energy,

$$\bar{\sigma}_{ij} = \frac{\int_{E_{\min}}^{E_{\max}} dE \sigma_{ijk}(E) \phi_k(E)}{\int_{E_{\min}}^{E_{\max}} dE \phi_k(E)} \quad (5.41)$$

where the limits of integration correspond to the three ranges in the summation. The constant, C , is the conversion to specific activity and is equal to unity for activity in Becquerels/cm³. The outer sum over index i is over the possible radionuclides and the sum over the index j represents the sums over the parent atoms of atomic density N_j (atoms/cm³) in air. The flux densities are, without further information, the average over some relevant spatial volume.

Adjustments for the presence of ventilation can be quite conveniently made by for a given radionuclide by using an effective decay constant, λ' , that includes the physical decay constant, λ , along with a ventilation term, r ,

$$\lambda' = \lambda + r, \quad (5.42)$$

$$\text{where } r = \frac{D}{V},$$

with D being the ventilation rate in air volume per unit time and V being the enclosure volume. Thus r is the number of air changes per unit time. The applicable differential equation with ventilation included is, then,

$$\frac{dn'}{dt} = -\lambda' n'(t) + N\sigma\phi. \quad (5.43)$$

$$\text{The solution is: } n'(t) = \frac{N\sigma\phi}{\lambda + r} \{1 - \exp[-(\lambda + r)t]\}. \quad (5.44)$$

So the specific activity is:

$$a'(t) = \lambda n'(t) = \frac{\lambda N\sigma\phi}{\lambda + r} \{1 - \exp[-(\lambda + r)t]\} \quad (5.45)$$

But $N\sigma\phi$ is just the saturation concentration, a_{sat} , without mixing. Hence, with mixing the saturation concentration, a'_{sat} is:

$$a'_{sat} = \frac{\lambda a_{sat}}{\lambda + r}. \quad (5.46)$$

The airborne radioactivity is of primary concern to workers who might enter the enclosure to perform maintenance activities. Since the principal radionuclides are of relative short half-life, the hazard is largely due to the "immersion" in a source of external dose rather than a gaseous ingestion hazard such as might be found in operations involving the processing of long-lived radioactive materials. Nevertheless, regulatory authorities, guided by ICRP and NCRP recommendations, have established quantities called "Derived Air Concentrations" (DAC) for radiation workers. DACs are based upon the receipt of 5000 mrem of dose equivalent if the entire working year (≈ 2000 hours) is spent working in a concentration corresponding to "1 DAC". A one DAC concentration is generally a quite large concentration that is rarely encountered in accelerator radiation

Chapter 5 Induced Radioactivity at Accelerators

environments. Similarly, for members of the general public, values of "Derived Concentration Guides" (DCGs) have been tabulated that would result in the receipt of 100 mrem of dose equivalent by an individual who spent all of the time in one year breathing such air. Table 5.6 gives representative values of these quantities based upon present U. S. Department of Energy Orders (DOE90) and Regulations (CFR93) along with some values determined for accelerator-produced radionuclides not included in the cited references that have been calculated by Höfert (Hö69). For some radionuclides commonly found at accelerators (CFR93) gives two values of DAC, one for air inhaled into the lungs and the other for immersion in an infinite cloud of γ -emitting radionuclides. The latter condition is more likely to be the dominant exposure mechanism due to activated air at accelerators. Not all radionuclides of concern in the air at accelerators are included in the U. S. Department of Energy tabulations and thus must be determined independently. Hence, the Höfert calculations are very important because they provide values for these accelerator-produced radionuclides. Also, Höfert recognized that such "immersion dose" is highly sensitive to the size of the cloud and that clouds of infinite extent are rare inside buildings at accelerators. He then calculated the equivalent of DACs for clouds of various sizes; Table 5.6 gives those for clouds of 4 meters radius that might be typical of an accelerator enclosure. For the general population, Höfert postulated an infinite cloud, since such exposure would presumably occur outdoors.

Table 5.6 DACs and DCGs (Air) for radiation workers and the general population. ($\mu\text{Ci}/\text{m}^3$)

Radionuclide	DAC-Radiation Worker 5 rem/year-40 hrs/week			DCG-General Population 0.1 rem/year-168 hrs/week	
	Inhaled Air (CFR93)	Immersion in infinite cloud (CFR93)	Immersion in 4 meter cloud (Ho69)	(DOE90)	(Ho69)
^3H	20			0.1	
^7Be	9			0.04	
^{11}C	200	4	59	1.0	
^{13}N		4	41		0.02
^{15}O		4	27		0.02
^{41}Ar		3	47		0.01
^{22}Na	0.3			0.001	

Propagation of Airborne Radioactivity-Tall Stacks

The other consideration concerning airborne radioactivity is that associated with the dose to members of the general public. The U. S. Environmental Protection Agency (EPA) has placed a 10 mrem/year limit on dose equivalent to members of the general public due to the operations of DOE facilities and has also placed stringent regulations on how such releases are to be measured (CFR90). The regulations prescribe the specific computer codes that must be used to calculate the dose to the public due from a given release point using a Gaussian plume model. Such computer modeling will not be described in detail here. Examples of such plume models are given in standard text books and the results

Chapter 5 Induced Radioactivity at Accelerators

depend on details of the meteorological conditions. Such concentrations can be estimated analytically using the so-called "Sutton's equation" to be described shortly. A good description that applies to rather tall (> 25 m) release points has been given by H. Cember (Ce69). The dispersion is mainly characterized by dilution of the radionuclides and their eventual return to ground level breathing zones. The meteorological conditions are of major importance and are illustrated in Fig. 5.8. Especially important are the stability classes:

stable: No heat is gained or lost by a parcel of air that rises and expands adiabatically with falling temperature. The adiabatic cooling with rise normally corresponds to a gradient of 5.4 °F/1000 ft (1 °C/100 meters) for dry air and 3.5 °F/1000 ft (0.6 °C/100 meters) for moist air. If the atmospheric temperature gradient is less than adiabatic, but still negative, stability is achieved because a rising parcel cools faster than its surroundings and then tends to sink. A sinking parcel is warmer than its surroundings and thus is less dense and tends to rise. This restricts the width of the plume and consequently decreases dilution.

inversion: If the temperature gradient is such that the temperature increases with height, then an inversion occurs. Rising effluent from a "stack" becomes much denser than its surroundings and thus sinks. The effluent is thus more limited in its ascent and this, too, serves to limit dilution.

superadiabatic: If the rate of decrease of temperature with elevation is greater than that in adiabatic conditions, an unstable condition results which promotes the vertical dispersion, and hence dilution. A rising parcel does not cool fast enough due to its expansion and therefore remains warmer and continues to rise. Likewise, a falling parcel continues to fall.

Table 5.7 gives certain parameters to be used in Sutton's equation as expressed by (Ce69) for tall stacks. In this table, the "chimney height" is the effective chimney height as calculated according to Eq. (5.48).

Table 5.7 Diffusion (C^2) and Stability (n) parameters for Sutton's Equation (Eq. 5.47). [Adapted from (Ce69).]

Lapse Rate	n	C^2			
		Chimney height (meters)			
		25	50	75	100
Superadiabatic	0.20	0.043	0.030	0.024	0.015
Stable	0.25	0.014	0.101	0.008	0.005
Moderate Inversion	0.33	0.006	0.004	0.003	0.002
Large Inversion	0.5	0.004	0.003	0.002	0.001

Chapter 5 Induced Radioactivity at Accelerators

Sutton's equation, as adapted here for consideration of short-lived radionuclides, is:

$$\bar{c}(x, y) = \frac{2Q}{\pi C^2 \bar{u} x^{2-n}} \exp\left\{-\frac{\lambda}{\bar{u}} \sqrt{x^2 + y^2}\right\} \exp\left\{-\frac{h^2 + y^2}{C^2 x^{2-n}}\right\} \quad (5.47)$$

where the exponential involving the decay constant λ conservatively allows for radioactive decay in transit for a particular radionuclide and;

$\bar{c}(x, y)$ is the average concentration (activity per m^3),

Q is the emission rate of activity per second,

(x, y) are coordinates to the point of measurement from the foot of the stack (meters);

x is along the centerline of the plume as determined by the wind direction (downwind), y is the transverse coordinate, and z , is the vertical coordinate,

\bar{u} is the mean wind speed, meters per second,

C is the virtual diffusion constant in lateral and vertical directions (see Table 5.7),

n is a dimensionless parameter related to the atmospheric conditions (Table 5.7),

h is the *effective* chimney height (if the gas has significant emission velocity) determined as follows from the actual chimney height h_a ;

$$h = h_a + d \left(\frac{v}{\bar{u}}\right)^{1.4} \left(1 + \frac{\Delta T}{T}\right). \quad (5.48)$$

In the above, h_a is the actual height in meters, d is the outlet diameter in meters, v is the exit velocity of the gas (meters/sec), and ΔT is the difference between the temperature of the gas and the ambient outdoor temperature divided by the absolute temperature of the gas, T .

Propagation of Airborne Radioactivity-Short Stacks

The above representation of Sutton's equation is a useful one where tall stacks are involved. However, at typical accelerator facilities it is uncommon for stacks to be as tall as 25 meters. Slade's treatise (Sl68) on the subject describes atmospheric releases of radionuclides. For purposes of this discussion, only steady state conditions continuous in time are treated here. In this treatment, the concentration as a function of coordinates (x, y, z) , defined as for the tall stacks, is given by a somewhat different formulation of Sutton's equation which uses the same coordinate system;

Chapter 5 Induced Radioactivity at Accelerators

$$\bar{c}(x, y, z) = \frac{Q}{2\pi\sigma_y\sigma_z\bar{u}} \left\{ \exp\left[-\frac{\lambda}{\bar{u}}\sqrt{x^2 + y^2}\right] \right\} \left\{ \exp\left(-\frac{y^2}{2\sigma_y^2}\right) \right\} \left\{ \exp\left[-\frac{(z-h)^2}{2\sigma_z^2}\right] + \exp\left[-\frac{(z+h)^2}{2\sigma_z^2}\right] \right\}. \quad (5.49)$$

For the common situation of interest where the receptor location of concern is at ground level ($z = 0$), this simplifies to

$$\bar{c}(x, y, 0) = \frac{Q}{\pi\sigma_y\sigma_z\bar{u}} \left\{ \exp\left[-\frac{\lambda}{\bar{u}}\sqrt{x^2 + y^2}\right] \right\} \left\{ \exp\left[-\left(\frac{y^2}{2\sigma_y^2} + \frac{z^2}{2\sigma_z^2}\right)\right] \right\}, \quad (5.50)$$

where the presence of the ground as a "barrier" to the flux is taken into account. In these equations, the quantity h is the elevation of the stack top above the ground in meters and $\sigma_y(x)$ and $\sigma_z(x)$ are the dispersion coefficients and have units of length (meters) and are implicitly functions of x . All other quantities are the same as given above for tall stacks. These variables are, of course, determined from the meteorological conditions.

Table 5.8 gives a scheme for classifying the meteorological conditions. The condition classification may then be used with the curves in Figs. 5.9 and 5.10 to determine the values of σ_y and σ_z as a function of the coordinate x .

Table 5.8 Relation of turbulence types to weather conditions. [Adapted from (SI68).]

A-Extremely unstable conditions		D-neutral conditions ^a			
B-Moderately unstable conditions		E-Slightly stable conditions			
C-Slightly unstable conditions		F-Moderately stable conditions			
Surface Wind Speed (m/sec)	Daytime insolation			Nighttime conditions	
	Strong	Moderate	Slight	Thin overcast or $\geq 4/8$ cloudiness ^b	$\leq 3/8$ cloudiness
<2	A	A-B	B		
2	A-B	B	C	E	F
4	B	B-C	C	D	E
6	C	C-D	D	D	D
>6	C	D	D	D	D

^aApplicable to heavy overcast, day or night

^bThe degree of cloudiness is defined as that fraction of the sky above the local apparent horizon which is covered by clouds.

Chapter 5 Induced Radioactivity at Accelerators

Airborne radioactivity emissions can be minimized by:

- limiting the ventilation rates during operations when people are not present in the enclosure,
- delaying the actual emissions by requiring long pathways to the ventilation "stacks", and
- minimizing air gaps in the beam.

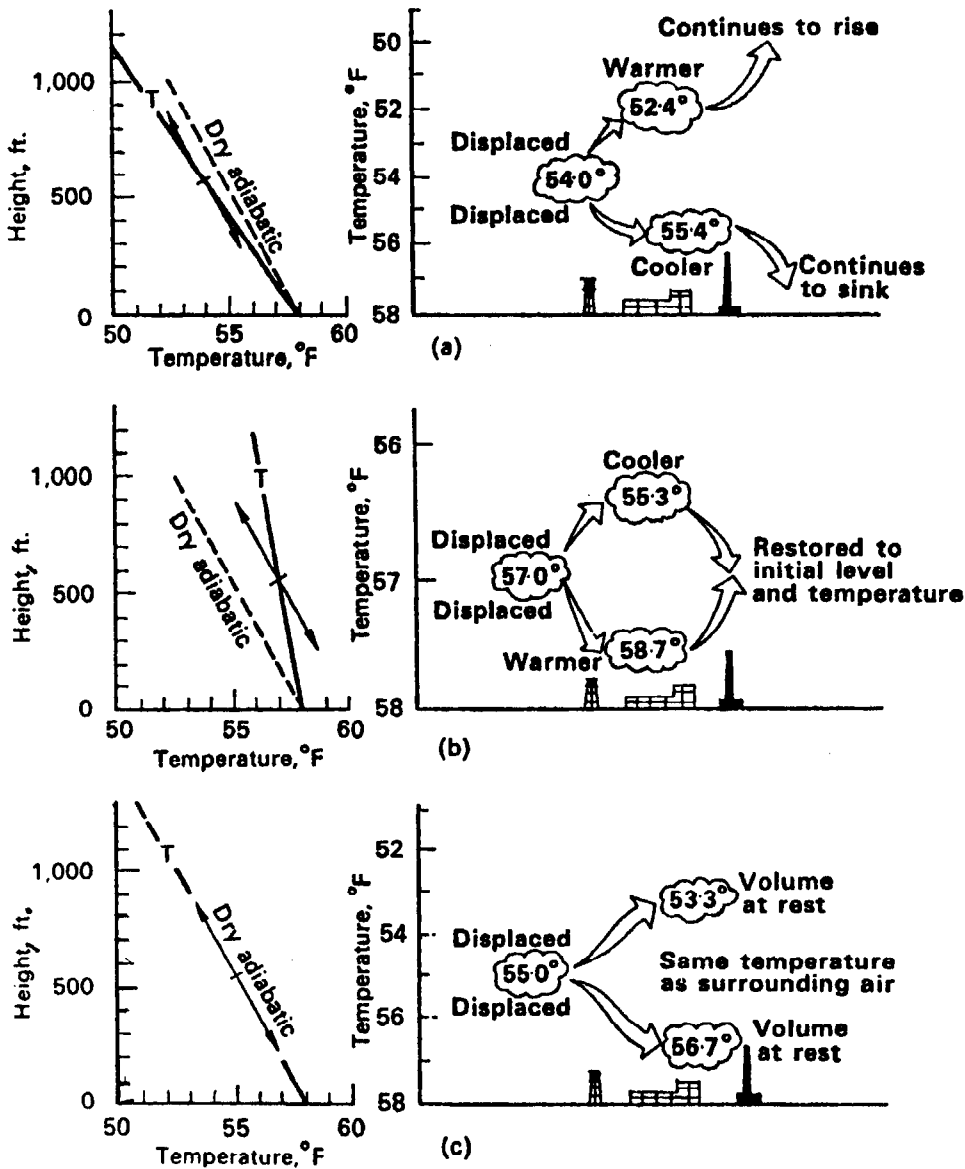


Fig. 5.8 Effect of atmospheric temperature gradient-or lapse rate- on a displaced volume of air for various conditions: **a** Unstable lapse rate; **b** Stable lapse rate; **c** Neutral lapse rate [Reproduced from (SI68).]

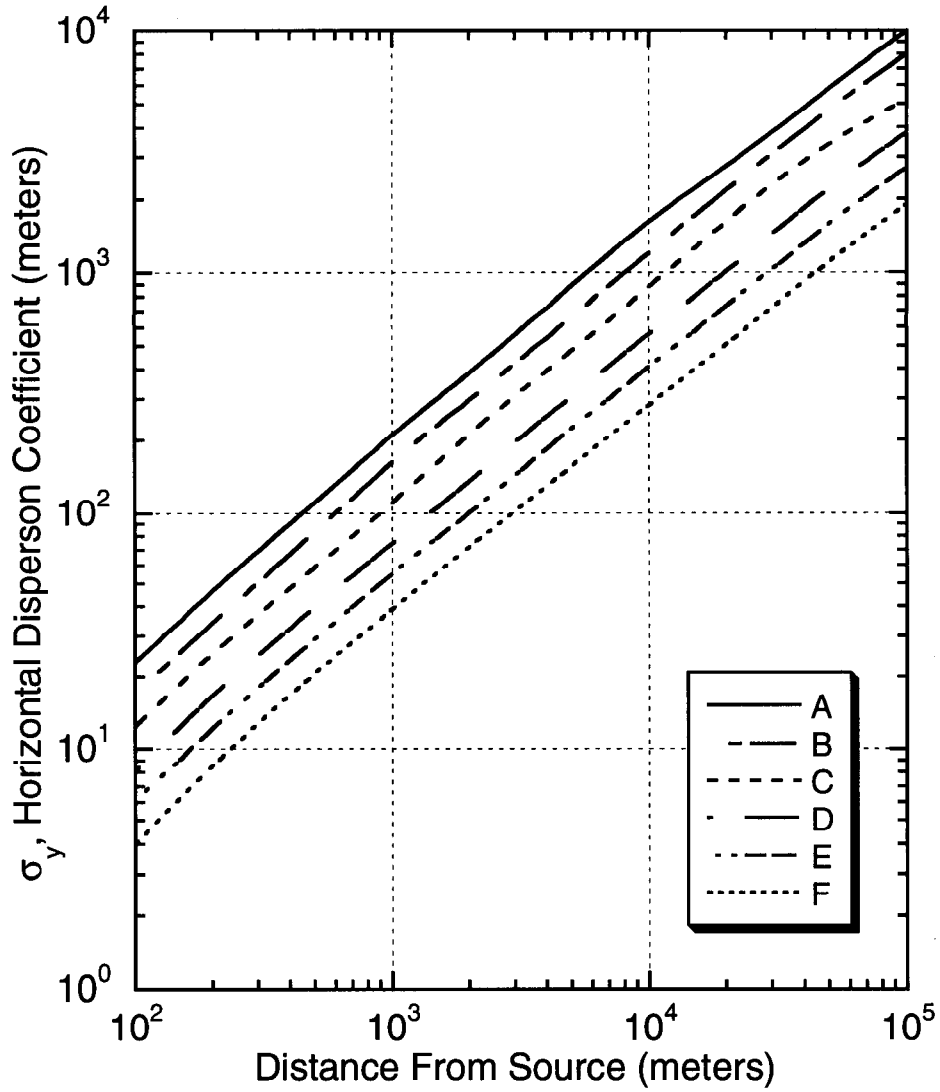


Fig. 5.9 Lateral diffusion, σ_y , as a function of downwind distance, x , source for turbulence types as defined in Table 5.8. [Adapted from (S168).]

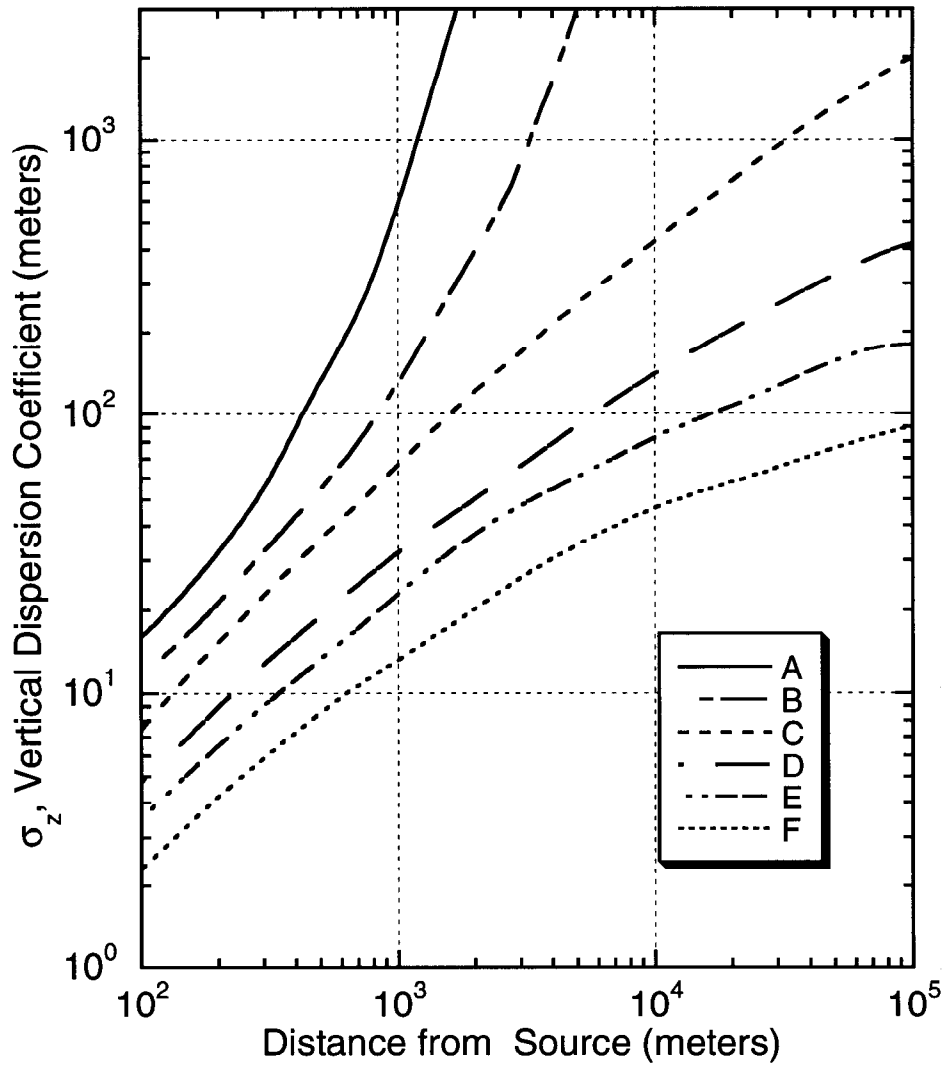


Fig. 5.10 Vertical diffusion, σ_z , as a function of downwind distance, x , from source for turbulence types as defined in Table 5.8. [Adapted from (S168).]

IV. Soil and Groundwater Activation

The protection of groundwater resources is a significant public concern that includes the need to assure protection of groundwater resources from contamination with radionuclides. In principal, radioactivity can be produced in both the earth itself and in the water it contains. In practice, it is not always a simple matter to separate these two sources. One could initiate calculations of groundwater activation at accelerators by starting from "first principles" and by using the activation formula. However, in practice such calculations have been done more frequently by analyzing results obtained using irradiated samples. The work of Borak, et al, (Bo72) is of singular importance in this regard. Borak et al. measured the radioactivity produced in soil by high energy hadrons by radiochemical analysis of soil samples irradiated near high energy synchrotrons; the 12 GeV Argonne ZGS and the 28 GeV Brookhaven AGS. The radionuclides ^3H , ^7Be , ^{22}Na , ^{45}Ca , ^{46}Sc , ^{48}V , ^{51}Cr , ^{54}Mn , ^{55}Fe , ^{59}Fe , and ^{60}Co were identified. Laboratory experiments were then performed to determine which radionuclides, and what fractions of them could be leached by water. This study determined macroscopic production cross sections and ion velocities relative to ground water flow in soil. Of these nuclides, only ^3H , ^{22}Na , ^{45}Ca , and ^{54}Mn were observed in leach waters. The ^3H was assumed to be all leachable and was measured by driving it out of the sample by baking. Radionuclides with half lives exceeding 15 days were the only ones considered. The results were based upon the elemental composition of soil given in Table 5.9.

Table 5.9 Composition of Soils Typical of the Fermilab site. [Adapted from Bo72].]

Elemental Composition of Soil		
Element	Z, Atomic Number	% by Weight
Silicon	14	14.47
Aluminum	13	2.44
Iron	26	1.11
Calcium	20	7
Magnesium	12	3.79
Carbon	6	5.12
Sodium	11	0.34
Potassium	19	0.814
Oxygen	8	≈ 64

The mean moisture percentage was $13.15 \pm 4.45 \%$ and the mean pH was 7.6 ± 0.1 .

The activities at saturation, A_i , are given (in Bq) by:

$$A_i = \phi \sum_j n_j \sigma_{ij} \quad (5.51)$$

where ϕ is the flux density, n_j is the number of target nuclei of the j^{th} nuclide per gram of the soil sample, and σ_{ij} is the effective cross section for the transformation from target nucleus j to radionuclide i . The sum is over the soil constituents. Borak, et al. were able to measure the summations on the right hand side of Eq (5.51) to determine the total

Chapter 5 Induced Radioactivity at Accelerators

macroscopic cross sections for each radionuclides of interest. Table 5.10 gives the results of the measurements of the macroscopic cross sections, Σ ($\text{cm}^2 \text{g}^{-1}$), for each of the radionuclides identified in the various types of soils analyzed.

Table 5.10 Macroscopic cross section for soil normalized to unit flux of hadrons with kinetic energies greater than 30 MeV. [Adapted from (Bo72).]

Nuclide	Glacial Till Σ ($\text{cm}^2 \text{g}^{-1}$)	Gray Sandy Clay Σ ($\text{cm}^2 \text{g}^{-1}$)	Red Sandy Clay Σ ($\text{cm}^2 \text{g}^{-1}$)	Gray Clay Σ ($\text{cm}^2 \text{g}^{-1}$)
⁷ Be	2.9×10^{-4}	3.7×10^{-4}	3.2×10^{-4}	2.7×10^{-4}
⁵¹ Cr	1.7×10^{-5}	3.7×10^{-5}	2.8×10^{-5}	3.1×10^{-5}
²² Na	2.1×10^{-4}	2.3×10^{-4}	2.0×10^{-4}	1.6×10^{-4}
⁵⁴ Mn	5.9×10^{-5}	4.1×10^{-5}	3.5×10^{-5}	3.7×10^{-5}
⁴⁶ Sc	3.0×10^{-5}	1.3×10^{-5}	9.6×10^{-6}	1.1×10^{-5}
⁴⁸ V	4.1×10^{-6}	1.1×10^{-5}	6.7×10^{-6}	7.4×10^{-6}
⁵⁵ Fe	9.3×10^{-5}	1.2×10^{-4}	7.0×10^{-5}	2.1×10^{-4}
⁵⁹ Fe	3.2×10^{-6}	1.7×10^{-6}	1.3×10^{-6}	1.6×10^{-6}
⁶⁰ Co	3.3×10^{-5}	1.4×10^{-5}	1.1×10^{-5}	1.3×10^{-5}
⁴⁵ Ca	1.6×10^{-4}	2.0×10^{-5}	3.0×10^{-5}	1.6×10^{-5}
³ H	8.2×10^{-4}	1.1×10^{-3}	3.3×10^{-4}	5.2×10^{-4}
³ H*	5.9×10^{-3}	5.9×10^{-3}	4.1×10^{-3}	4.4×10^{-3}

*Activity and cross sections per gram of water in soil.

Some comments should be made with respect to the leachabilities found for each of the four nuclides identified as *leachable* by Borak et al.:

- ³H- The leaching process was able to collect all the tritium measured by the bake-out process. The average value of the macroscopic cross section in soil was found to be $5.1 \times 10^{-3} \text{ cm}^2/\text{g}$ of water. An important conclusion is that the tritium will migrate with the same velocity as any other water in the soil.
- ²²Na- Typically 10-20 % of this nuclide was leachable. On average, it appeared that the migration velocity of this nuclide is approximately 40% of that of water through the soil due to ion exchange processes.
- ⁴⁵Ca- At most 5 % of this nuclide was leached from the soil. The migration velocity was determined to be extremely small.
- ⁵⁴Mn- At most 2 % of this nuclide was leached from the soil. It was determined that this nuclide will not migrate significant distances.

One can thus calculate the quantities of radionuclides that might pose a risk to groundwater in the environs of an accelerator. This can be done, as demonstrated by Gollon (Go78), by performing, for example, Monte-Carlo calculations in which the total stars (or inelastic interactions above some threshold) produced in some volume of earth shielding are determined. The total number of atoms, K_i , of the i^{th} nuclide that can be produced per star in that same volume would then be given by

$$K_i = \frac{\Sigma_i}{\Sigma_{ne}}, \quad (5.52)$$

where Σ_i is, as above, the macroscopic cross section (cm^2/gram) for the i^{th} radionuclide and Σ_{ne} is the total macroscopic nonelastic cross section (cm^2/gram) for soil. Gollon quotes a value of $\Sigma_{ne} = 1.1 \times 10^{-2} \text{ cm}^2/\text{gm}$ for soil. Thus, a calculation of total stars in some soil volume per unit time can be taken directly from the Monte-Carlo calculations. Gollon used the following values for ^3H and ^{22}Na as selected from Borak's paper for soils peculiar to Fermilab (glacial till):

$$K_3 = \frac{8.2 \times 10^{-4}}{1.1 \times 10^{-2}} = 0.075 \quad (5.53a)$$

$$K_{22} = \frac{2.1 \times 10^{-4}}{1.1 \times 10^{-2}} = 0.02. \quad (5.53b)$$

One can then calculate the total number of atoms of radionuclides produced during some time interval in some volume by simply multiplying these factors by the number of stars (or nonelastic interactions) in the same volume. The number of atoms then can be converted to activity using the decay constant. The above values of K_i are applicable to soils such as those found at Fermilab. For other soil compositions one may need to use cross sections for producing the radionuclides of interest in various target elements and perform an integration over the energy spectrum of incident hadrons. Figures 5.11 and 5.12 give cross sections for producing these two radionuclides by interactions of hadrons with the various elements comprising soil. The results for ^3H are for incident neutrons and follow the method specified by Konobeyev and Korovin (Ko93). It is anticipated that the results for protons do not differ greatly from these except at the lower energies just above the reaction thresholds. The results for ^{22}Na are due to Van Ginneken (Va71).

The quantity of ultimate concern, of course, is the resultant concentration water. The water would be a groundwater resource that might well be protected by regulatory authorities. The regulations may well differ between different governing jurisdictions. Such requirements were generally not developed for application to the operations of particle accelerators and generally need to be well-understood by the designers of accelerator facilities. The United States Environmental Protection Agency (CFR76) limits such concentrations to those that would produce a dose equivalent of 4 mrem/year and specifically gives a limit of 20 pCi/ml for tritium as a legal limit. An explicit limit for ^{22}Na is not specified by EPA. The U.S. Department of Energy (DOE90) specifies limits using a more up-to-date dosimetry methodology that results in a limit of 80 pCi/ml for ^3H and 0.4 pCi/ml for ^{22}Na . At any rate, the concentration in the water must satisfy the following inequality:

$$\sum_i \frac{C_i}{C_{\text{max},i}} \leq 1. \quad (5.54)$$

Chapter 5 Induced Radioactivity at Accelerators

The numerator in the summation is the concentration of some particular nuclide i while the denominator is the allowed limit. The methods for calculating these concentrations will vary with the regulatory authority and the "conservatism" of the institution. The most conservative assumption is to assume that saturation values of production are reached. This is equivalent to assuming that the accelerator will operate "forever" and that the water in its vicinity never moves. It is questionable that the water in such a medium would be considered to comprise a groundwater resource. However, for this static case, the activity concentration C_i of radionuclide i , under such conditions can be calculated by means of following formula:

$$C_i \text{ (pCi / ml)} = \frac{N_p K_i L_i S_{ave}}{1.17 \times 10^6 \rho w_i} \{1 - \exp(-t_{irrad} / \tau_i)\} \exp(-t_c / \tau_i). \quad (5.55)$$

In this formula,

N_p is the number of incident particles delivered per year,

K_i is as above,

L_i is the fraction of the radionuclide of interest that is leachable,

S_{ave} is the average star density (stars cm^{-3}) in the volume of interest per incident particle,

ρ is the density of the medium (g cm^{-3}),

w_i is the mass (grams) of water per unit mass (grams) of medium required to leach some specified fraction of the leachable radioactivity and is, thus, linked to the value of L_i .

t_{irrad} is the irradiation time,

t_c is the "cooling" time once the irradiation is suspended, and

τ_i is the mean life of the i^{th} radionuclide.

The constant in the denominator contains the unit conversions to yield pCi/ml.

For a given medium, the ratio L_i/w_i should be determined by measurements specific to the local media. Also, for the truly static situation, the product, $\rho w_i = p$, the porosity of the material. This provides a means by which "worst case" estimates may be made. For realistic estimates some method of taking into account water movement must be used.

At Fermilab, a simple model allowing some movement and further dilution of water has been employed for many years (Go78). In this model, the vertical migration of water was assumed to be 2.2 meters per year. In the standard clays present, this migration velocity is conservative, but likely high by at least an order of magnitude. Its use crudely allowed for the presence of cracks and fissures through which more rapid propagation of water might be possible. The tritium vertical velocities are taken to be this value while the results obtained in (Bo72) were used to obtain a reduced value of about one m/year for ^{22}Na . Only the leachable fraction of the ^{22}Na according to (Bo72) is included. The procedure, then, allowed for decay during the downward migration of the total inventory of radionuclides produced in one year, integrated over the entire volume of the irradiated material, to the highest aquifer below the location of the irradiation. At that point, it was

Chapter 5 Induced Radioactivity at Accelerators

assumed that the radionuclides are rapidly transported to a shallow well where it is assumed that the flow of water collecting the radionuclides is entirely used by a single user who consumes a very low value of 150 liters per day. This value was taken from minimal values achieved by municipalities that needed to ration public water consumption during severe drought conditions. Thus the annual production, as transported vertically, is diluted into the $5.5 \times 10^7 \text{ cm}^3/\text{year}$ that this represents. This simple model is generally conservative but does, in fact, neglect that fact that the water movement may not be uniform from year-to-year. It also does not use the fact that the radionuclides are initially distributed over a considerable volume as they are produced. It is clear that better methods may be needed and a new model has been developed for use at Fermilab (Ma93). A new model used at Fermilab calculates the production of the radionuclides of concern in accordance with Eq. (5.55). The result, then, provides an initial concentration that is available for further migration, decay, and dilution. The concentration after migration is, then, calculated by using up-to-date modeling techniques to calculate the reduction in the concentration due to dilution, diffusion, and radioactive decay. At the point of concern, usually the location of an aquifer suitable for consumption as a water supply, the concentrations calculated are then substituted into Eq. (5.54) in order to determine if a shielding design is adequate.

To do these calculations properly requires a detailed knowledge of the media involved. Some principles will be given here. In situations where a definite potential gradient, often called the **hydraulic gradient**, dh/dx , is applied to water in a medium, the rate of flow is said to be **advective**. Under such conditions and in situations where only one dimensional coordinate is important, the average linear velocity (or seepage velocity), v , is given by the application of **Darcy's Law** as (Fe 88),

$$v = \frac{K}{p} \frac{dh}{dx} \quad (5.56)$$

where p is the **effective porosity** of the material and represents the volume fraction of the material that is available to water movement. More complicated situations involving two and three dimensions are addressable using the mathematical language of vector calculus. The effective porosity is essentially equal to the pore volume of the material for soils but for consolidated materials it does not include sealed pores through which movement is not allowed. The derivative is the gradient of the hydraulic head in the material. K in this equation represents the **hydraulic conductivity**. This quantity is a function of the material and its moisture content. All of the factors in this equation can, and generally should, be determined empirically for the medium and location under consideration. Typical values of K are given in Table 5.11 and have been given by Batu (Ba98).

Chapter 5 Induced Radioactivity at Accelerators

Table 5.11 Examples of typical values of hydraulic conductivity [Adapted from (Ba98).]

Group	Porous Materials	Range of K values (cm s^{-1})
Igneous Rocks	Weathered granite	$(3.3 - 52) \times 10^{-4}$
	Weathered gabbro	$(0.5 - 3.8) \times 10^{-4}$
	Basalt	$(0.2 - 4250) \times 10^{-6}$
Sedimentary Materials	Sandstone (fine)	$(0.5 - 2250) \times 10^{-6}$
	Siltstone	$(0.1 - 142) \times 10^{-8}$
	Sand (fine)	$(0.2 - 189) \times 10^{-4}$
	Sand (medium)	$(0.9-567) \times 10^{-4}$
	Sand (coarse)	$(0.9- 6610) \times 10^{-4}$
	Limestone and dolomite	$(0.4 -2000) \times 10^{-7}$
	Karst limestone	$(1- 20000) \times 10^{-4}$
	Gravel	$(0.3 - 31.2) \times 10^{-1}$
	Silt	$(0.09-7090) \times 10^{-7}$
	Clay	$0.1 - 47) \times 10^{-8}$
Metamorphic Rocks	Schist	$(0.002 - 1130) \times 10^{-6}$

Darcy's law can, then, be used to determine the rate of migration of a contaminant, in this case, radioactivity from one point to another. During the time of migration, the concentration would be reduced due to radioactive decay. This method would be particularly applicable to determining the migration of contamination due to spills. One often encounters the problem of calculating the concentration of radionuclides at some location as a function of time during, or after, a period of irradiation comparable to the mean lives of the radionuclides of concerns. At a given location in such a medium, denoted by the coordinate x , one needs to solve the following continuity equation which is an extension of Eq. (5.4),

$$\frac{\partial C_i}{\partial t} + v \frac{\partial C_i}{\partial x} + \lambda_i C_i(x, t) = \frac{L_i}{w'_i} Q_i(x, t), \quad (5.57)$$

where all constants are as in Eq. (5.55) except that λ_i is the decay constant of the i^{th} radionuclide, x is the spatial coordinate, t is the time, w'_i is the water content of the media per unit volume of media. The quantity $Q_i(x, t)$ represents the production the i^{th} radionuclide and is equivalent to the factor $N_p S_{ave} / (1.17 \times 10^6 \rho)$. It includes any time-dependence in the delivery of beam. The middle term in the left-hand side of the equation takes care of movement from a point of one concentration to another at the seepage velocity v of the particular radionuclide i . One can often describe the spatial dependence of the production factor as,

$$Q_i(x, t) = Q_{oi}(t) \exp(-\xi x), \quad (5.58)$$

where the spatial distribution of the production follows an exponential dependence as is typical in a large shield.

Mokhov (Mo97) has solved this equation for the typical initial conditions of $C_i(x, 0) = 0$ and $x \geq 0, t \geq 0$.

Chapter 5 Induced Radioactivity at Accelerators

In general, $C_i(x,t) = \frac{L_i}{w_i} \int_0^t dt' Q_i(x - vt', t') \exp(-\lambda t')$ (5.59a)

and for an exponential spatial dependence as in Eq. (5.58) this becomes:

$$C_i(x,t) = Q_{oi}(t) \frac{L_i}{w_i} \frac{1}{\eta_i} \exp(-\xi x) [\exp(\eta_i \tau) - 1]$$

with $\eta_i = \xi v - \lambda_i$,
 $\tau = t$ for $t < x/v$, and
 $\tau = x/v$ for $t \geq x/v$. (5.59b)

$C_i(x,t)$ has a maximum at $x_{i,max}$ given by,

$$x_{i,max} = -\frac{v}{\lambda_i} \frac{\ln\left(\frac{\xi v}{\lambda_i}\right)}{1 - \frac{\xi v}{\lambda_i}}. \quad (5.60).$$

In situations where the seepage velocity is very slow, diffusion becomes the dominant mechanism for water flow and dilution. Mathematically, a second partial derivative with respect to the spatial coordinate is added to Eq. (5.57). Example solutions are provided by Fetter (Fe88). Modern computer programs have been written to address this topic such as the one produced by Sudicky, et al. (Su88).

Jackson has estimated the dilution for a shallow uncased well in an aquifer a distance r from a beam loss point also in the aquifer (Ja87). The loss point was assumed to be within the drawdown zone of the well. This was performed for a simple geology that involved a single uniform stratum of earth above some level of impervious stratum. Fig. 5.13 taken shows the situation described by this model. Here, a given well is modeled by using the profile of depth of water $h(r)$ at distance r from the well. $h(r)$ is determined by the depth of a test well at radius r from the well under consideration and represents the hydraulic potential. The well is assumed to supply a volume Q of water per day. The flux of water is determined by the gradient relation which is equivalent to Darcy's Law,

$$S_r = k \frac{dh(r)}{dr} \quad (5.61)$$

where S_r is the inward flux at radius r and k is a constant with dimensions of volume per unit time per unit area and is characteristic of the soil.

Conservation of water yields the steady-state equation:

$$Q = 2\pi r h(r) S_r = 2\pi r k h \frac{dh}{dr} = \pi k \frac{d(h^2)}{d(\ln r)}. \quad (5.62)$$

The quantity $2\pi r h \frac{dh}{dr}$ corresponds to the rate of change of volume of the cylindrical shell of height h ("the head") with respect to r .

Chapter 5 Induced Radioactivity at Accelerators

This equation has the solution:

$$Q \ln \left(\frac{r}{r_o} \right) = \pi k \{ h^2(r) - h_o^2 \} \quad (5.63)$$

where r_o is the radius of the well and h_o is the height of water above the impervious stratum at the well. If H is the depth of the impervious layer below the water table unperturbed by the wells, the radius of influence R of the well can be defined by the relation:

$$\ln \frac{R}{r_o} = \frac{\pi k \{ H^2 - h_o^2 \}}{Q} \quad (5.64)$$

However, the detailed solution is not necessary.

Now, suppose that there is a well a distance r away from the region of deposition of radioactivity near an accelerator. We also assume that the activation zone lies below the water table and that the deposition region lies within the radius of influence of the well. This assumption leads to higher concentrations than would be obtained if the activation zone were totally, or partially, above the water table. The amount of activity drawn into the well is determined by the rate of pumping Q and the necessary total flow through a cylinder of radius r and height $h(r)$ as we have seen. Let ΔV be the volume of soil yielding Q gallons of water. The cylindrical shell providing this amount of water will be of radial thickness Δr , where $\Delta V = 2\pi r h(r) \Delta r$. The fraction F of the volume of activity included in this shell can be said to be given by:

$$F = \frac{\Delta r}{t} = \frac{2\pi r h \Delta r}{2\pi r h t} = \frac{\Delta V}{2\pi r h t} \quad (5.65)$$

provided that $\Delta r < t$.

If the activated region contains leachable activity, A (either total activity or that of a particular radionuclide of interest), the corresponding specific activity, a , in water drawn from the well is thus given by:

$$a = F \frac{A}{Q} = F \frac{A}{p \Delta V} = \left[\frac{\Delta V}{2\pi r h t} \right] \frac{1}{p} \left[\frac{1}{\Delta V} \right] A = \frac{1}{2\pi r t D} \frac{f}{p} A \quad (5.66)$$

where $f = D/h$ is the fraction of the total height of the cylindrical shell occupied by the activated region and p is the **porosity** of the soil. The pumping volume Q is implicit in f . Porosity values vary considerably but in general are in the range,

$$0.2 < p < 0.35. \quad (5.67)$$

Thus, this formula may be used to obtain an estimate of the specific activity as a function of distance from the well, although it is perhaps not too useful for applications to beam losses far from the well. By definition, $f \leq 1$ and the lower value of porosity can be used to obtain upper limit estimates of the concentration. It must be emphasized that this model depends upon uniformity of water conduction by the strata. The presence of "cracks", of course, can provide much more rapid movement that is not well-described by this simple model.

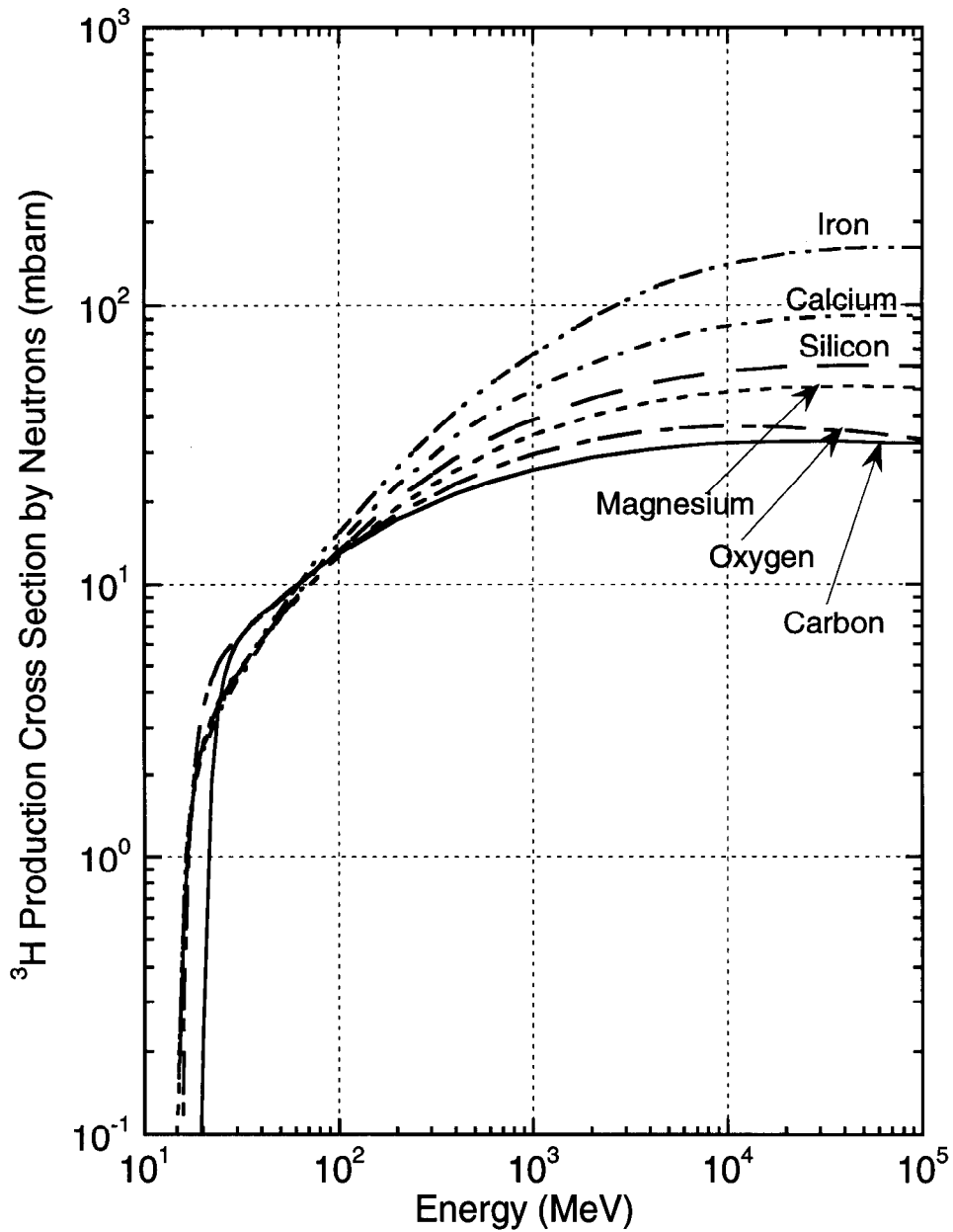


Fig. 5.11 Cross sections for the production of ^3H due to neutron bombardment of materials commonly found in soil and rock as a function of neutron energy. The calculations have been performed following the method of Konobeyev and Korovin (Ko93). Results for aluminum are quite similar to those found for silicon and the results for sodium are quite similar to those found for magnesium.

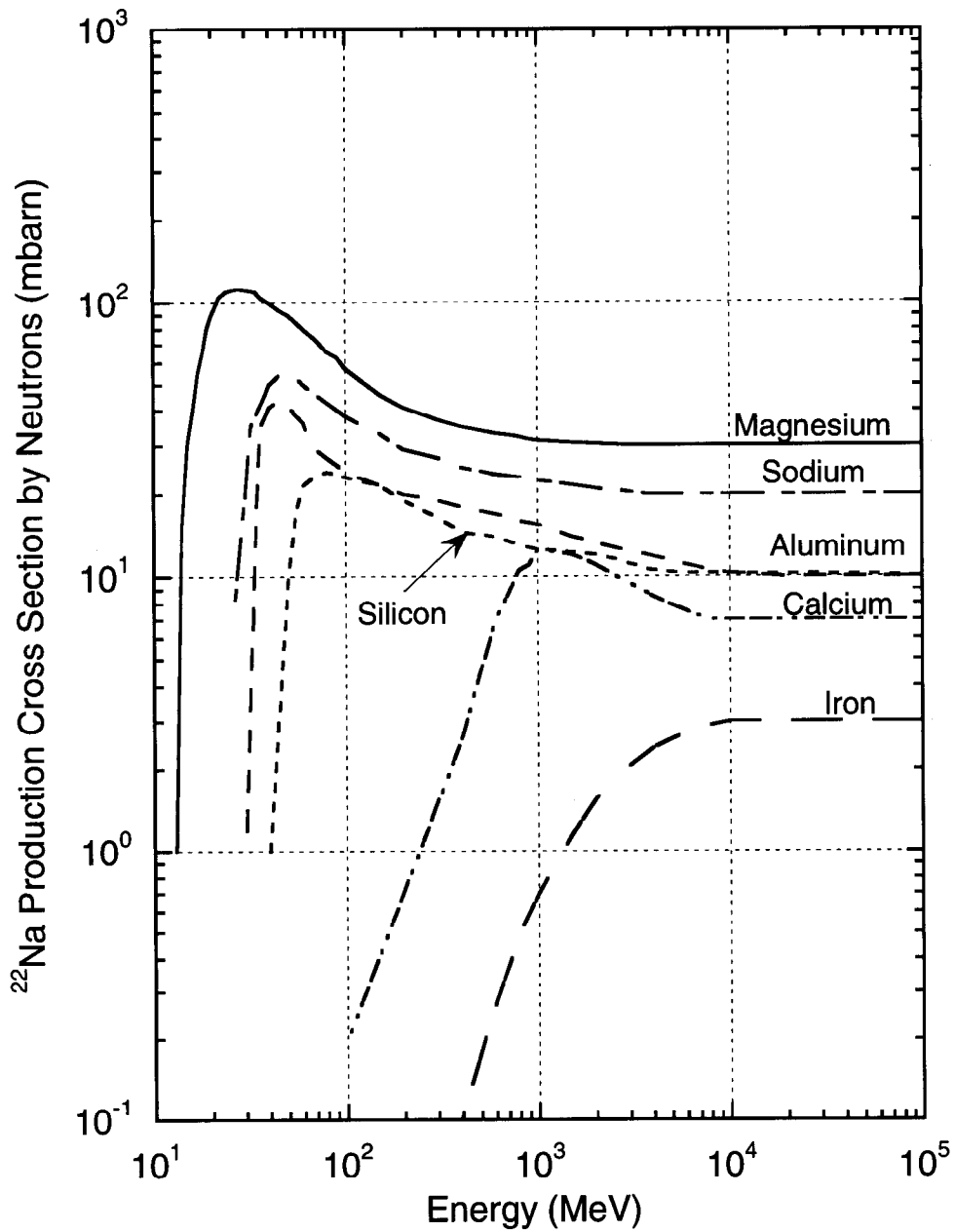


Fig. 5.12 Cross sections for the production of ^{22}Na due to neutron bombardment of materials commonly found in soil and rock as a function of neutron energy. Results for potassium are quite similar to those found for calcium. [Adapted from (Va71)].

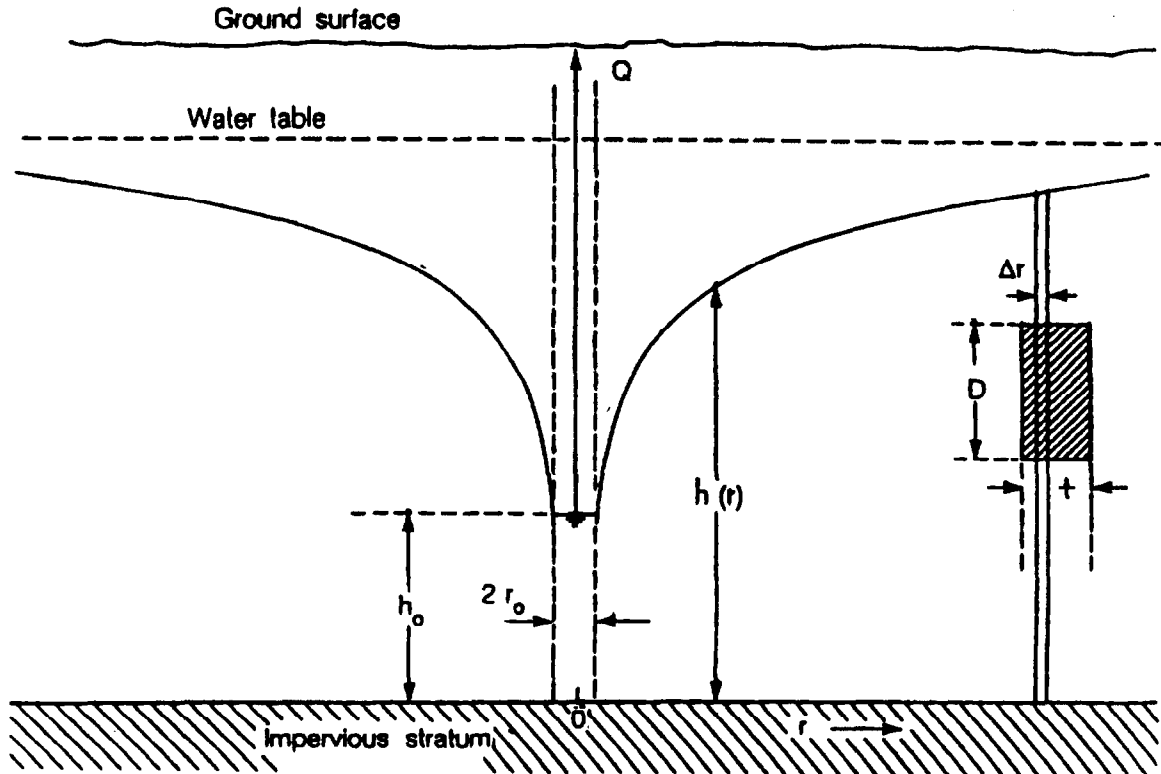


Fig. 5.13 Hydrogeological model of a shallow well in proximity to an accelerator tunnel where a beam loss occurs. The radioactivated region is represented in cross section by the shaded rectangle to the right. h represents the elevation of the water table above the impervious stratum as a function of r while the water table is distance H of the water table above the impervious stratum where the former is not perturbed by wells. [Adapted from (Ja87).]

Chapter 5 Induced Radioactivity at Accelerators

References

- (Ar69a) T. W. Armstrong and R. G. Alsmiller, Jr., "Calculation of the residual photon dose rate around high energy proton accelerators", Nucl. Sci. and Eng. 38 (1969) 53-62.
- (Ar69b) T. W. Armstrong and J. Barish, "Calculation of the residual photon dose rate due to the activation of concrete by neutrons from a 3-GeV photon beam in iron," in *Proceedings of the second international conference on accelerator radiation dosimetry and experience*, (Stanford, CA 1969).
- (Ar73) T. W. Armstrong and R. G. Alsmiller, Jr, "Calculations of the residual photon dose rate around high energy proton accelerators", Nucl. Sci. Eng. 38 (1973) 53-62.
- (Ba98) V. Batu, *Aquifer hydraulics* (John Wiley and Sons, Inc., New York, 1998).
- (Ba69) M. Barbier, *Induced radioactivity*, (North-Holland Publishing Company, Amsterdam and London, Wiley Interscience Division, John Wiley and Sons, Inc, New York, 1969).
- (Bo72) T. B. Borak, M. Awschalom, W. Fairman, F. Iwami, and J. Sedlet, "The underground migration of radionuclides produced in soil near high energy proton accelerators", Health Physics 23 (1972) 679-687.
- (Bu89) S. W. Butala, S. I. Baker, and P. M. Yurista, " Measurements of radioactive gaseous releases to air from target halls at a high-energy proton accelerator", Health Physics 57 (1989) 909-916.
- (Ce69) H. Cember, *Introduction to health physics*, (Pergamon Press, New York, 1969).
- (CFR76) United States Code of Federal Regulations, Title 40, Part 141.16, "National primary drinking water standard for beta- and gamma- emitting radionuclides", 1976.
- (CFR89) United States Code of Federal Regulations, Title 40, Part 61, Subpart H, "National emissions standard for hazardous air pollutants (NESHAP) for the emission of radionuclides other than radon from Department of Energy Facilities", 1989.
- (CFR93) United States Code of Federal Regulations, Title 10 Part 835, "Occupational radiation protection at department of energy facilities", 1993.

Chapter 5 Induced Radioactivity at Accelerators

- (Co78) B. L. Cohen, "Nuclear cross sections", *Handbook of radiation measurement and protection, Section A: Volume I Physical science and engineering data*, A. Brodsky, editor (CRC Press, Inc., West Palm Beach, Florida, 1978).
- (Co96) J. D. Cossairt, "On residual dose rate within particle accelerator enclosures", *Health Phys.* 71 (1996) 315-319.
- (Co98) J. D. Cossairt, "Rule of thumb for estimating groundwater activation from residual dose rates", Fermilab Environmental Protection Note No. 15, June 1998.
- (DOE90) U. S. Department of Energy Order 5400.5, "Radiation protection of the public and the environment" (1990).
- (Fe88) C. W. Fetter, *Applied hydrogeology* (Merrill Publishing Company, Columbus, OH, 1988).
- (Ga73) T. A. Gabriel and R. T. Santoro, "Photon dose rates from the interactions of 100 GeV protons in iron and iron-lead beam stops", *Part. Acc.* 4 (1973) 169-186.
- (Go76) P. J. Gollon, "Production of radioactivity by particle accelerators", Fermilab Report TM-609 and also *IEEE Trans. Nucl. Sci.* NS 23 No. 4 (1976) 1395-1400.
- (Go78) P. J. Gollon, "Soil activation calculations for the anti-proton target area", Fermilab Report TM-816 (1978)
- (Hö69) M. Höfert, "Radiation hazard of induced activity in air as produced by high energy accelerators", in *Proceedings of the second international conference on accelerator radiation dosimetry and experience*, (Stanford, CA 1969).
- (Ja87) J. D. Jackson, editor, G. D. Murdock, D. E. Groom, J. R. Sanford, G. R. Stevenson, W. S. Freeman, K. O'Brien, R. H. Thomas, "SSC Environmental Radiation Shielding", SSC Central Design Group Report SSC-SR-1026 (1987).
- (Ko93) A. Yu. Konobeyev and Yu. A. Korovin, "Tritium production in materials from C to Bi irradiated with nucleons of intermediate and high energies", *Nucl. Instrm. and Meth. in Phys. Res.* B82 (1993) 103-115.

Chapter 5 Induced Radioactivity at Accelerators

- (Ma93) A. J. Malensek, A. A. Wehmann, A. J. Elwyn, K. J. Moss, and P. M. Kesich, "Groundwater migration of radionuclides at Fermilab", Fermilab Report TM-1851 (August, 1993).
- (Mo97) N. Mokhov, private communication (1997).
- (NC99) R. H. Thomas (chair), W. R. Casey, N. Rohrig, J. D. Cossairt, L. A. Slaback, K. O'Brien, G. B. Stapleton, and W. P. Swanson, National Council on Radiation Protection and Measurements (NCRP), NCRP Report 51 (Revised)--in preparation.
- (Pa58) H. W. Patterson and R. Wallace, "A method of calibrating slow neutron detectors, Lawrence Radiation Laboratory Report UCRL-8359 (1958).
- (Pa73) H. W. Patterson and R. H. Thomas, *Accelerator health physics*, Academic Press, New York, 1973.
- (Sl68) D. A. Slade, Editor, *Meteorology and atomic energy* (U. S. Atomic Energy Commission, Office of Information Services, July, 1968).
- (Su65) A. H. Sullivan and T. R. Overton, "Time variation of the dose-rate from radioactivity induced in high-energy particle accelerators", *Health Physics* 11 (1965) 1101-1105.
- (Su88) E. A. Sudicky, T. D. Wadsworth, J. b. Kool, and P. S. Huyakorn, "PATCH 3D; Three dimensional analytical solution for transport in a finite thickness aquifer with first-type rectangular patch source", Prepared for Woodward-Clyde Consultants, Inc., Waterloo, Ontario, Canada, University of Waterloo, 1988.
- (Sw90) W. P. Swanson and R. H. Thomas, "Dosimetry for radiological protection at high energy Particle Accelerators", Chapter 1 in *The Dosimetry of ionizing radiation*, Volume III (Academic Press, 1990).
- (Th88) R. H. Thomas and G. R. Stevenson, "Radiological safety aspects of the operation of proton accelerators", Technical Report No. 283, International Atomic Energy Agency, Vienna, 1988.
- (Tu84) J. W. N. Tuyn, R. Deltenre, C. Lamberet, and G. Roubaud, "Some radiation aspects of heavy ion acceleration", Proc. 6th Int. Cong. International Radiation Protection Association, Berlin (1984) 673.
- (Va71) A. Van Ginneken, " Na^{22} production cross section in soil", Fermilab Report TM-283, January 1971.

Chapter 5 Induced Radioactivity at Accelerators

- (Va93) K. Vaziri, V. Cupps, D. Boehnlein, D. Cossairt, A. Elwyn, and T. Leveling, "AP0 stack monitor calibration", Fermilab Radiation Physics Note #106, May 1993.
- (Va94) K. Vaziri, V. R. Cupps, D. Boehnlein, D. Cossairt, and A. Elwyn, "A detailed calibration of a stack Monitor used in the measurement of airborne radionuclides at a high energy proton accelerator", Fermilab Report FERMILAB-Pub-96/037, 1996.

Chapter 5 Induced Radioactivity at Accelerators

Problems

1. A copper beam stop has been bombarded with high energy hadrons for 30 days and exhibits a dose rate of 100 mrem/hr at 1 meter away 1 day after the beam is turned off. Maintenance work needs to be scheduled in the vicinity within the next 6 months. Using both Gollon's Rule # 3 (as derived by Sullivan and Overton) and the Barbier Danger parameter curves, predict the cooling curve and determine when the dose rate is less than a 20 mrem/hr maintenance work criteria. Make a table of dose rate versus cooling time in days for both methods. How well do the two methods agree? (Hint: Use initial value of the dose rate to scale values of D .)
2. A 100 GeV beam (10^{12} protons/second) strikes the center of a large solid iron cylinder 30 cm in radius for 30 days. Use the star density curves from the Chapter 3 (Fig 3.12) and the " ω " factors calculated by Gollon to estimate the residual dose rate after 1 day cooldown at contact with the side of the cylinder in the "hottest" spot. Using Gollon's third rule, how long must the repair crew wait to service this time in a contact radiation field of absorbed dose rate < 10 rad/hr?
3. A copper target is bombarded with high energy protons such that 10 stars per incident proton are produced. If the incident beam is 10^{11} p/s, what is the specific activity (average) of ^{54}Mn that is produced after two years of operation? ^{54}Mn has a high energy spallation production cross section of about 20 mb in Cu. The target is a cylinder, 10 cm radius by 15 cm long. The half-life of ^{54}Mn is 312 days. Express the answer in both Bq/cm³ and Ci/cm³. (Hint: This problem is best if the calculation is done at saturation and then corrected for the non-infinite irradiation time. Also, one needs to use the inelastic cross section given, for example, in Chapter 3.)
4. A 20 m long air gap has a beam of 10^{12} p/s of high energy protons passing through it. First, calculate the production rate of ^{11}C in the gap at equilibrium if one approximates air in the gap by nitrogen and assumes $\sigma(^{11}\text{C}) = 10$ mb. Assume that there are no significant losses of beam by interaction after checking to see that this assumption is, in fact, true. Table 1.2 should contain helpful information.
 - a) If the air gap is in a $10 \times 10 \times 20$ meter³ enclosure with no ventilation, calculate the equilibrium concentration of ^{11}C in the room (in units of $\mu\text{Ci}/\text{m}^3$) assuming extremely rapid mixing (i.e., no time allowed for decay while mixing occurs) of the enclosed air. Compare the concentration with the derived air concentration values in Table 5.6 and calculate, using simple scaling, the dose equivalent to a worker who spends full time in this room. (This is a purely hypothetical scenario due to the much larger hazards due to such an intense direct beam!)
 - b) Calculate the concentration if two (2) air changes/hr are provided.

Chapter 5 Induced Radioactivity at Accelerators

- c) Assume the exhaust of the ventilation described in part "b" is through a 10 cm radius stack 25 m tall. Calculate the air speed in the stack, and the emission rate Ci/s. Then using Cember's version of Sutton's equation for tall stacks to estimate the concentration directly downwind at ground level, and hence the dose equivalent 1 km away with moderately stable meteorological conditions and an average wind speed of 10 km/hr.
- d) Perform the same calculation requested in "c" using the more general version of Sutton's equation appropriate to short stacks and assume the stack height to be 3 meters. All other conditions of the problems are the same as in "c".
5. In soil conditions similar to those at Fermilab, a volume of soil around a beam dump approximately 10 m wide by 10 m high by 20 m long is the scene of a star production rate (averaged over the year) of 0.02 star/proton at a beam intensity of 10^{12} protons/sec.
- a) Calculate the annual production of ^3H ($t_{1/2} = 12.3$ years), the saturated activity (in Bq & Ci), and the average saturated specific activity in the above volume's water (assume 10% water content by volume).
- b) Use the older "Fermilab Model" to calculate the concentration at the nearest well. Assume the activation region (beam loss point) is 50 m above the aquifer and the usual migration velocities.
- c) "Conservatively" apply the "Jackson Model" to estimate the concentration at a well 100 meters distant from the center of the activation region.